

SIP-BMM: Constructing the Capability–Efficiency Pareto Set for LLMs via Structural Importance Prior Bayesian Model Merging

Kesheng Chen, Yamin Hu, Zhenqian Zhu, Yiya Diao, Wenjian Luo

Guangdong Provincial Key Laboratory of Novel Security Intelligence Technologies,
School of Computer Science and Technology, Harbin Institute of Technology, Shenzhen, China
luowenjian@hit.edu.cn

Abstract

Constructing a Pareto set is pivotal for navigating the capability–efficiency trade-offs in Large Language Models (LLMs). However, existing merging techniques remain inadequate: coarse-grained, model-level methods yield only a sparse set of suboptimal solutions, while fine-grained, layer-wise optimization suffers from the curse of dimensionality under expensive evaluations. We propose Structural Importance Prior Bayesian Model Merging (SIP-BMM), a framework that makes layer-wise Pareto-set construction tractable by *explicitly modeling which layers matter*. Specifically, SIP-BMM derives a **Structural Importance Prior (SIP)** from layer-wise task-vector differences between base and expert models, and uses this prior to guide Sparse Axis-Aligned Subspace Bayesian Optimization (SAASBO) toward a low effective-dimensional subspace. Intuitively, SIP steers the optimizer to spend most trials on a small set of influential layers while largely ignoring layers that exhibit minimal task-relevant shifts. This importance-aware search preserves layer-wise control while substantially reducing sample complexity. The process is automated within an evolutionary loop driven by Log-Noisy Expected Hypervolume Improvement (q NEHVI). Experiments show that SIP-BMM discovers a stronger and denser Pareto front than competitive baselines, enabling agile model selection under diverse operational constraints. Code is available at: <https://github.com/MiLab-HITSZ/2026-SIPBMM>.

1 Introduction

Large language models (LLMs) have revolutionized natural language processing by exhibiting remarkable reasoning abilities, often facilitated by chain-of-thought (CoT) prompting [Wei *et al.*, 2022]. However, extended reasoning sequences incur significant computational costs, including latency, token usage, and resource consumption [Sui *et al.*, 2025]. In real deployments, these costs directly translate into throughput degradation and higher serving expense, motivating a careful balance between *capability* (e.g., reasoning acc-

curacy) and *efficiency* (e.g., compute or output length). Model merging has therefore emerged as a promising technique to amalgamate specialized models—e.g., fusing a “Thinking” expert with a base model into a unified entity that balances these competing objectives—without retraining from scratch [Wu *et al.*, 2025; Team *et al.*, 2025].

Constructing a Pareto set is essential for navigating the complex trade-offs between capability and efficiency in LLMs. Nevertheless, prevalent merging techniques predominantly focus on coarse-grained, model-level fusion, which we find yields only a limited number of suboptimal solutions. This limitation stems from the fact that a single global interpolation weight cannot capture heterogeneous layer-wise specialization: different layers often contribute unevenly to reasoning, instruction following, and efficiency-related behaviors. As a result, model-level merging typically produces only a few discrete operating points and struggles to provide a continuous spectrum of capability–efficiency trade-offs, restricting flexibility in practical deployment. Moreover, these approaches often rely on manual hyperparameter tuning (e.g., sparsity thresholds or sign-agreement rules), making it difficult to systematically and reproducibly explore the trade-off landscape.

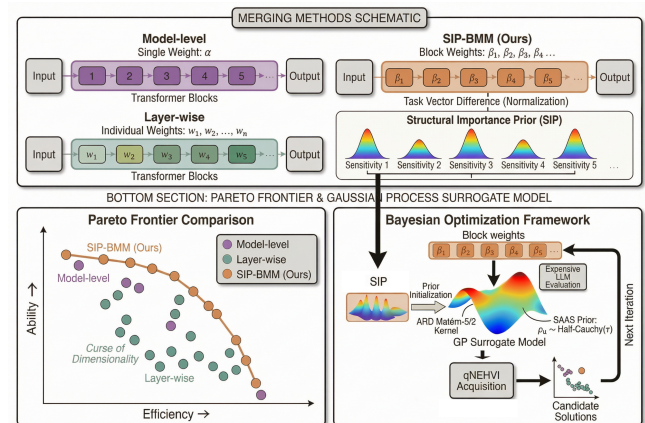


Figure 1: Schematic comparison of Pareto fronts constructed via different merging strategies. SIP-BMM leverages structural importance priors to efficiently navigate the high-dimensional layer-wise search space, achieving a denser and stronger front than coarse model-level and naive layer-wise approaches.

Conversely, recent layer-wise optimization methods attempt to increase granularity by searching for per-layer mixing coefficients using evolutionary computation or Bayesian optimization [Akiba *et al.*, 2025; Li *et al.*, 2025]. While offering finer control, this strategy faces a critical scalability barrier as LLM depth increases: the decision space grows linearly with the number of layers, quickly reaching dozens (or more) of continuous dimensions. Under realistic evaluation budgets—where each candidate merge must be validated on expensive benchmarks—this “curse of dimensionality” makes naive high-dimensional search sample-inefficient. In particular, surrogate-based optimization with standard Gaussian Processes (GPs) becomes computationally burdensome and statistically brittle in high dimensions, which can prevent the optimizer from reliably identifying a high-quality Pareto front.

To address these challenges, we propose SIP-BMM (Structural Importance Prior Bayesian Model Merging), an automated evolutionary multi-objective framework for constructing the LLM Pareto set via *layer-wise* merging. SIP-BMM injects architectural structure into the search by using a *Structural Importance Prior (SIP)*—computed from layer-wise task-vector shifts between base and expert models—to guide a Sparse Axis-Aligned Subspace Bayesian optimization (SAASBO) surrogate. This design biases the optimizer toward low effective dimensionality, enabling sample-efficient exploration in high-dimensional layer-wise spaces. To ensure stable and fair optimization across heterogeneous metrics, we further adopt a normalized objective formulation anchored by established base and expert models. The overall process is driven by the q -Expected Hypervolume Improvement (qEHVI) acquisition function to efficiently refine and diversify the Pareto frontier under limited evaluation budgets.

Experiments show that SIP-BMM discovers a stronger and denser Pareto front than competitive model-level merging baselines, enabling rapid model selection under diverse operational constraints.

Contributions. Our contributions are as follows:

- **Framework.** We present SIP-BMM, an automated evolutionary multi-objective framework for constructing the capability–efficiency Pareto set via *layer-wise* LLM merging.
- **Method.** We propose a Structural Importance Prior (SIP) computed from layer-wise task-vector differences and use it to initialize the SAAS-GP lengthscale priors, enabling sample-efficient Bayesian optimization in a 36-dimensional layer-wise search space.
- **Evidence.** We show on GPQA-Diamond and AIME25 that SIP-BMM yields a stronger and denser Pareto front (higher hypervolume and coverage) than competitive model-level merging baselines under a matched real evaluation budget.

2 Background

2.1 Model Merging Methods

Model merging combines the parameters of multiple neural networks into a unified model $\mathcal{M}^{(\text{merge})}$ to amalgamate complementary capabilities without retraining from scratch [Yang *et al.*, 2024]. Given a set of K models $\{\mathcal{M}^{(1)}, \dots, \mathcal{M}^{(K)}\}$ derived from a common base model $\mathcal{M}^{(\text{base})}$, the objective is to find an effective fusion of their task vectors or weights.

Early parameter-level strategies focus on mitigating interference during fusion. Weight averaging [Utans, 1996] and task arithmetic [Ilharco *et al.*, 2022] provide basic interpolation and vector manipulation. More advanced methods like TIES-Merging [Yadav *et al.*, 2023], DARE-Merging [Yu *et al.*, 2024], and DELLA-Merging [Deep *et al.*, 2024] introduce sparsification, sign agreement, and pruning to reduce redundancy and conflicts. While computationally efficient, these methods predominantly operate at a coarse, model-level granularity and often rely on handcrafted hyperparameters, making them insufficient for systematically exploring the LLM capability–efficiency trade-off surface.

To automate the merging process, evolutionary computation-based methods have recently emerged. TIES-DARE [Akiba *et al.*, 2025] utilizes CMA-ES [Hansen *et al.*, 2003] to search for layer-wise mixing coefficients, though it primarily focuses on single-objective optimization. MO-MM [Li *et al.*, 2025] formulates merging as a multi-objective problem, employing Bayesian optimization with the Log-Noisy Expected Hypervolume Improvement (q NEHVI) acquisition function [Daulton *et al.*, 2020] to identify Pareto-optimal solutions across conflicting tasks. However, as LLM depth increases, these layer-wise approaches encounter the curse of dimensionality: the resulting high-dimensional search space renders standard Gaussian Process surrogates computationally intractable and prone to overfitting. This motivates a framework that maintains fine-grained control while exploiting structural priors to navigate high-dimensional spaces efficiently.

2.2 Multiobjective Optimization

Multiobjective optimization (MO) aims to find a set of solutions that represent optimal trade-offs among conflicting objectives [Deb *et al.*, 2002]. The central concept is the Pareto front: solutions for which no objective can be improved without degrading at least one other objective. A multiobjective optimization problem (MOP) is commonly stated as optimizing a vector of objective functions

$$F(X) = (f_1(X), f_2(X), \dots, f_m(X)),$$

subject to constraints, where X is a decision vector in the feasible region. Key concepts include:

- **Pareto dominance:** X dominates Y if $f_i(X) \leq f_i(Y)$ for all i and $f_j(X) < f_j(Y)$ for at least one j (for minimization; inequalities reverse for maximization).
- **Pareto optimality:** a solution is Pareto optimal if no other feasible solution dominates it.
- **Pareto set (PS):** the set of all Pareto-optimal solutions in decision space.
- **Pareto front (PF):** the image of the PS in objective space, representing the optimal trade-offs.

When objective evaluations are expensive (as in LLM merging, where each candidate may require multiple benchmark runs), Bayesian optimization (BO) is a common choice.

BO fits a probabilistic surrogate (often a GP) and selects new candidates via an acquisition function that trades off exploration and exploitation. In the multiobjective setting, acquisition functions such as $q\text{EHVI}/q\text{NEHVI}$ [Daulton *et al.*, 2020] are widely used because they directly target Pareto-front quality by maximizing (noisy) expected hypervolume improvement, support batch (parallel) candidate selection, and naturally encourage diverse solutions along the frontier.

3 Methodology

3.1 Problem Formulation

Our goal is to construct an LLM Pareto set that captures trade-offs between reasoning capability and efficiency, enabling rapid deployment of models under different operational constraints without retraining. The Pareto set can further be combined with routing strategies or user preferences to select an appropriate model for a given scenario.

Multi-objective model fusion. We formulate model fusion as a multi-objective optimization problem with K objectives:

$$\max F(\mathcal{M}_{\text{merge}}) = (f_1(\mathcal{M}_{\text{merge}}), \dots, f_K(\mathcal{M}_{\text{merge}})), \quad (1)$$

where f_k denotes the k -th capability-related objective (higher is better).

We define the evaluation benchmark set for the k -th capability as $Q^{(k)}$, and its corresponding benchmark score set as $S^{(k)}$. Let $\mathcal{M}_{\text{expert}}^{(k)}$ be the model specialized for the k -th capability, and $\mathcal{M}_{\text{base}}^{(k)}$ be the corresponding base reference model used for normalization. We define $Q^{(k)} = \{q_1^{(k)}, q_2^{(k)}, \dots, q_n^{(k)}\}$, where $q_n^{(k)}$ is the n -th benchmark for the k -th capability. Similarly, $S^{(k)} = \{s_1^{(k)}(\mathcal{M}_{\text{merge}}), \dots, s_n^{(k)}(\mathcal{M}_{\text{merge}})\}$, where $s_n^{(k)}$ is the score of $\mathcal{M}_{\text{merge}}$ on the n -th benchmark.

Normalized objectives. We compute the normalized objective for the k -th capability as:

$$f_k(\mathcal{M}_{\text{merge}}) = \sum_{s^{(k)} \in S^{(k)}} \left(\frac{s^{(k)}(\mathcal{M}_{\text{merge}}) - s^{(k)}(\mathcal{M}_{\text{base}}^{(k)})}{s^{(k)}(\mathcal{M}_{\text{expert}}^{(k)}) - s^{(k)}(\mathcal{M}_{\text{base}}^{(k)})} \right). \quad (2)$$

Layer-wise merging parameterization. To achieve fine-grained control over behavior, we perform interpolation at the layer level, assigning independent weights to each Transformer layer. Let the decision vector be $\mathbf{x} \in [0, 1]^D$ with $D = L$ (one scalar per layer). For the (two-model) case, \mathbf{x} directly specifies the layer-wise interpolation weights; for the multi-expert case, \mathbf{x} can be mapped to simplex weights by a normalization operator (details omitted as not the focus).

Concretely, we write:

$$\begin{aligned} \mathcal{M}_{\text{merge}} &= \text{Layer-Wise-Merge}(\{\mathcal{M}_i\}; \mathbf{x}), \\ \mathbf{x} &= (x_1, \dots, x_L), \quad x_l \in [0, 1], \quad l = 1, \dots, L, \end{aligned} \quad (3)$$

and the resulting merged model is evaluated by $F(\mathcal{M}_{\text{merge}}(\mathbf{x}))$ through Eq. (2).

3.2 Importance-Aware SAASBO

To scale optimization to the full layer-wise search space while maintaining sample efficiency, we propose an Importance-Aware SAASBO strategy. This framework integrates our Structural Importance Prior (SIP) with the Sparse Axis-Aligned Subspace BO (SAASBO) surrogate [Eriksson and Jankowiak, 2021]. In our setting, the decision vector assigns one mixing weight per Transformer layer; therefore the search space has dimension $D = L = 36$.

Task vector extraction. For each expert model $\mathcal{M}^{(i)}$ and the base model $\mathcal{M}_{\text{base}}$, we extract layer-wise task vectors $TV_l^{(i)} \in \mathbf{R}^{d_{\text{param}}}$:

$$TV_l^{(i)} = \mathcal{M}_l^{(i)} - \mathcal{M}_{\text{base},l}, \quad l = 1, \dots, L. \quad (4)$$

Functional difference quantification. We compute the layer-wise difference Diff_l to measure functional divergence of each layer across specialized models:

$$\text{Diff}_l = \sum_{i=1}^N \left\| TV_l^{(i)} - \frac{1}{N} \sum_{j=1}^N TV_l^{(j)} \right\|_p. \quad (5)$$

Sensitivity mapping. We normalize differences into an importance score $\mathcal{I}_d = \text{Norm}(\text{Diff}_d) \in [0, 1]$ and map \mathcal{I}_d to initial lengthscales $\ell_d^{(0)}$ via a piecewise function Φ :

$$\ell_d^{(0)} = \Phi(\mathcal{I}_d) = \begin{cases} 0.5, & \text{if } \mathcal{I}_d > 0.9 \text{ (Critical)} \\ 1.0, & \text{if } 0.8 < \mathcal{I}_d \leq 0.9 \text{ (Important)} \\ 5.0, & \text{if } \mathcal{I}_d \leq 0.7 \text{ (Stable)} \end{cases} \quad (6)$$

SAAS GP surrogate (per objective). Following [Williams and Rasmussen, 2006], we use an ARD Matérn-5/2 kernel to model each objective $y_k(\mathbf{x}) := f_k(\mathcal{M}_{\text{merge}}(\mathbf{x}))$ (Eq. (2)):

$$\begin{aligned} k(\mathbf{x}, \mathbf{x}') &= \sigma_f^2 \left(1 + \sqrt{5}r + \frac{5}{3}r^2 \right) \exp(-\sqrt{5}r), \\ \text{where } r &= \sqrt{\sum_{d=1}^D \frac{(x_d - x'_d)^2}{\ell_d^2}}. \end{aligned} \quad (7)$$

To enforce sparsity in high dimensions, we adopt the hierarchical SAAS prior [Eriksson and Jankowiak, 2021] on inverse squared lengthscales $\rho_d = 1/\ell_d^2$:

$$\tau \sim \text{Half-Cauchy}(\alpha), \quad \rho_d \sim \text{Half-Cauchy}(\tau), \quad d = 1, \dots, D. \quad (8)$$

By initializing the NUTS sampler [Hoffman and Gelman, 2014] with SIP-derived $\ell_d^{(0)}$, we warm-start exploration in architecturally significant regions.

3.3 Optimization Framework

Bayesian optimization loop. We optimize in the decision space $\mathbf{x} \in [0, 1]^D$, where each \mathbf{x} defines a merged model $\mathcal{M}_{\text{merge}}(\mathbf{x})$ (Eq. (3)) and an objective vector $\mathbf{y}(\mathbf{x}) = (y_1(\mathbf{x}), \dots, y_K(\mathbf{x}))$ with $y_k(\mathbf{x}) = f_k(\mathcal{M}_{\text{merge}}(\mathbf{x}))$ (Eq. (2)).

At iteration t , we fit a multi-output surrogate (implemented as K independent SAAS GPs for simplicity) on $\mathcal{D}_t = \{(\mathbf{x}_i, \mathbf{y}_i)\}_{i=1}^{n_t}$. We then select a batch of q candidates by maximizing the Log-Noisy Expected Hypervolume Improvement ($q\text{NEHVI}$) acquisition function [Daulton *et al.*, 2022].

q NEHVI. We adopt the q NEHVI acquisition function from prior work [Daulton *et al.*, 2022]. Let \mathcal{P}_t be the observed nondominated set and $\mathbf{r} \in \mathbb{R}^K$ a reference point. For q new objective vectors \mathbf{Y} , the hypervolume improvement (HVI) is

$$\text{HVI}(\mathbf{Y}; \mathcal{P}_t, \mathbf{r}) = \text{HV}(\mathcal{P}_t \cup \mathbf{Y}; \mathbf{r}) - \text{HV}(\mathcal{P}_t; \mathbf{r}). \quad (9)$$

For a candidate batch $\mathbf{X} = \{\mathbf{x}^{(i)}\}_{i=1}^q$ with $\mathbf{y}(\mathbf{x}) = (f_1(\mathcal{M}_{\text{merge}}(\mathbf{x})), \dots, f_K(\mathcal{M}_{\text{merge}}(\mathbf{x})))$ (Eq. (2)), q NEHVI is

$$\alpha_{q\text{NEHVI}}(\mathbf{X}) = \mathbb{E} \left[\text{HVI}(\mathbf{Y}(\mathbf{X}); \tilde{\mathcal{P}}_t, \mathbf{r}) \right], \quad (10)$$

where $\tilde{\mathcal{P}}_t$ is obtained by sampling noisy training outcomes from the GP posterior and taking the nondominated subset. We estimate and optimize $\alpha_{q\text{NEHVI}}$ via Monte-Carlo sampling with the log-stabilized implementation of [Daulton *et al.*, 2022]. Further implementation details are provided in supplementary material.

Solution selection. After obtaining the LLM Pareto set, we compute cosine similarity between normalized objective vectors \mathcal{Y}_P of Pareto solutions and a user-defined preference vector, then select the best overall model from the Top- K solutions with the highest cosine similarity (details omitted).

The overall optimization process is summarized in Algorithm 1.

Algorithm 1 The SIP-BMM Optimization Framework

```

Input: Expert models  $\{\mathcal{M}^{(i)}\}$ , base model  $\mathcal{M}_{\text{base}}$ , initial points  $N_0$ , iterations  $T$ , batch size  $q$ 
Output: Final Pareto set  $\mathcal{X}_{\text{final}}$  and Pareto front  $\mathcal{Y}_{\text{final}}$ 
// 1. Prior Extraction
Compute  $\text{Diff}_l$  for all layers  $l \in \{1, \dots, L\}$  using Eq. (5)
Initialize SIP lengthscales  $\ell_d^{(0)} \leftarrow \Phi(\text{Norm}(\text{Diff}_d))$  using Eq. (7)
// 2. Initialization
 $\mathcal{X}_0 \leftarrow \text{SobolSamples}(N_0)$ 
 $\mathcal{Y}_0 \leftarrow \text{EvaluateObjectives}(\mathcal{X}_0, \{\mathcal{M}^{(i)}\}, \mathcal{M}_{\text{base}})$ 
// 3. Importance-Aware BO Loop
for  $t = 0$  to  $T - 1$  do
  Fit SAAS GP with SIP:  $GP_t \leftarrow \text{FitSAAS}(\mathcal{X}_t, \mathcal{Y}_t, \ell_d^{(0)})$ 
   $\mathcal{X}_{\text{new}} \leftarrow \text{OptimizeAcquisition}(q\text{NEHVI}, GP_t, q)$ 
   $\mathcal{Y}_{\text{new}} \leftarrow \text{EvaluateObjectives}(\mathcal{X}_{\text{new}})$ 
   $\mathcal{X}_{t+1} \leftarrow \mathcal{X}_t \cup \mathcal{X}_{\text{new}}; \mathcal{Y}_{t+1} \leftarrow \mathcal{Y}_t \cup \mathcal{Y}_{\text{new}}$ 
end for
 $(\mathcal{X}_P, \mathcal{Y}_P) \leftarrow \text{GetParetoFront}(\mathcal{X}_T, \mathcal{Y}_T)$ 
 $(\mathcal{X}_{\text{final}}, \mathcal{Y}_{\text{final}}) \leftarrow \text{SelectSolution}(\mathcal{X}_P, \mathcal{Y}_P)$ 

```

4 Experimental Setup

4.1 Models and Benchmarks

We formulate the optimization problem with two conflicting objectives: reasoning capability $f_{\text{reasoning}}$ and model efficiency $f_{\text{efficient}}$. Our goal is to simultaneously improve reasoning performance and computational efficiency by fusing a specialized “Thinking” model $\mathcal{M}_{\text{think}}$ with an efficiency-oriented “Instruct” model $\mathcal{M}_{\text{instruct}}$.

We employ rigorous benchmarks including GPQA-Diamond [Rein *et al.*, 2024] and AIME25. The specific model parameter settings and definitions are summarized in Table 1.

Reasoning capability. We select a post-trained thinking model (e.g., Qwen3-4B-Thinking [Yang *et al.*, 2025]) as the expert. Reasoning is assessed using GPQA-Diamond and AIME25, with mean accuracy as the metric.

Model efficiency. We designate the post-trained instruct model (e.g., Qwen3-4B-Instruct [Yang *et al.*, 2025]) as the efficiency expert, given its optimization for concise generation. Efficiency is quantified by the average output token count on the same benchmarks; lower is better.

Table 1: Multi-objective Model Interpolation Parameter Settings

OBJECTIVE	REASONING	EFFICIENCY
EXPERT MODEL	THINKING MODEL	INSTRUCT MODEL
BASE MODEL	INSTRUCT MODEL	THINKING MODEL
METRIC	MEAN ACCURACY (↑)	MEAN TOKEN COUNT (↓)
BENCHMARKS	{GPQA-DIAMOND, AIME25}	{GPQA-DIAMOND, AIME25}

To streamline fusion and evaluation, we interpolate only these two models. For objective normalization, we set the “base” reference for each objective to be the opposing expert model (e.g., Instruct serves as the base for reasoning, and Thinking serves as the base for efficiency).

4.2 Baselines

We evaluate SIP-BMM against five state-of-the-art model-level merging methods: (1) Task Arithmetic [Ilharco *et al.*, 2022]; (2) TIES-Merging [Yadav *et al.*, 2023]; (3) DARE-Merging [Yu *et al.*, 2024]; (4) Breadcrumbs [Davari and Belilovsky, 2024]; and (5) DELLA [Deep *et al.*, 2024]. Detailed formulations are provided in the supplementary material.

4.3 Experimental Settings

We evaluate SIP-BMM along three axes: granularity necessity, baseline comparison, and ablation analysis.

Granularity comparison. To verify the necessity of layer-wise optimization, we construct solution sets using varying granularities: (1) model-level (a single global weight); (2) block-wise (9 and 18 blocks); and (3) layer-wise (independent weights for all 36 layers). For block-wise merging, we partition layers into K blocks using a *hybrid* Fisher-Jenks-style dynamic programming algorithm based on layer-wise task-vector difference magnitudes: it jointly encourages within-block homogeneity (variance) while balancing the total “difference mass” across blocks (sum deviation), so that highly active deep layers can be isolated instead of being diluted by many stable shallow layers. Full formulation and implementation details are provided in supplementary material.

Baseline comparison. We compare SIP-BMM against all model-level baselines (Task Arithmetic, TIES, DARE, Breadcrumbs, DELLA). For SIP-BMM, we set initial samples $N_0 = 8$ and run for $T = 20$ iterations with batch size $q = 4$, resulting in a total of $B = N_0 + Tq = 88$ real evaluations.

Fair evaluation budget for model-level baselines. To ensure a fair comparison, all model-level merging baselines are allocated the same number of *real* model evaluations as SIP-BMM, i.e., $B = N_0 + Tq$ (here, $B = 88$). This budget counts the initialization evaluations plus all subsequent true evaluations during the iterative process.

Adaptive grid search under a fixed budget. Under this fixed budget, model-level baselines are executed via an adaptive grid search whose grid resolution is determined by the available budget and the length of each search interval. For Task Arithmetic (TA), the entire budget is used to grid-search a single interpolation weight $\lambda \in [0.05, 0.95]$. For baselines with an additional density hyperparameter, we grid-search two variables: the interpolation weight $\lambda \in [0.05, 0.95]$ and the density $\delta \in [0.7, 0.9]$. Given a total of B evaluations, we allocate grid points to λ and δ proportionally to their interval lengths, using a 9:2 split between λ and δ . We then evaluate the Cartesian grid exhaustively until the budget is consumed.

Ablation study. To isolate the contribution of the Structural Importance Prior (SIP), we compare: (1) SIP-BMM (SAASBO + SIP) and (2) vanilla SAASBO (without SIP initialization). All configurations use the same evaluation budget.

For all experiments, inference parameters follow the official recommended settings for Qwen3 [Yang *et al.*, 2025], and all optimization runs use a fixed seed for reproducibility.

5 Results and Analysis

5.1 The Necessity of Layer-wise Granularity

Figure 2 and Table 2 illustrate Pareto fronts and summary metrics obtained with different merging granularities, ranging from model-level grid search to block-wise and finally to full layer-wise (36 dimensions) optimization. We observe a consistent trend: as the number of independent weight parameters increases, the Pareto front shifts toward improved trade-offs, indicating gains in both reasoning capability and token efficiency.

Table 2: Summary metrics across different merging granularities.

GRANULARITY	HV VALUE	COVERAGE	PARETO #
LAYER-WISE	1.322373	9/11	10
BLOCK-WISE (N=18)	1.364006	1/13	9
BLOCK-WISE (N=9)	1.290996	0/13	14
MODEL-LEVEL	1.270630	3/13	13

As summarized in Table 2, the layer-wise approach achieves the highest coverage (9/11), indicating superior approximation of the optimal trade-off surface. This suggests LLM capabilities are distributed heterogeneously across layers; hard block partitioning reduces dimensionality but can obscure layer-specific contributions. These results motivate scaling optimization to the full layer-wise space using SIP-BMM. Detailed metrics are provided in the supplementary material.

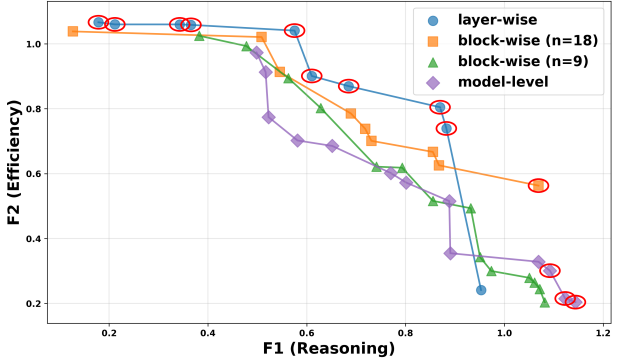


Figure 2: Distribution of merged models in objective space (f_1 vs. f_2).

Critical Observation: Searching for model-level fusion weights via fine-grained grid search is insufficient to uncover the true Pareto frontier available from merging models. Introducing fine-grained weight settings, particularly **layer-wise strategies**, is essential to unlock the full potential of the capability-efficiency trade-off.

Intuition: why finer granularity helps mostly in the middle. Beyond the overall improvement, we observe a consistent pattern in Figure 2: increasing the optimization granularity yields the largest gains for solutions in the *intermediate* trade-off region, while the differences near the two extremes are comparatively small. A plausible explanation is that extreme points are often dominated by candidates whose fusion weights are close to degenerate patterns (e.g., $\lambda \approx 0$ or $\lambda \approx 1$, or layer weights that are almost all near 0/1), effectively collapsing to “almost-efficiency” or “almost-ability” models. Such solutions have relatively simple, low-complexity weight structures and can therefore be approximated well even with coarse model-level or block-wise parameterization. In contrast, mid-front solutions typically require more heterogeneous, layer-dependent combinations to balance capability and efficiency, i.e., a higher-complexity composition of weights that coarse granularity cannot express. This observation reinforces our motivation: to explore a sufficiently diverse Pareto set and extract informative trade-off profiles for deployment, fine-grained (ideally layer-wise) merging is necessary.

Having established that layer-wise granularity is necessary, we next compare SIP-BMM against existing baselines.

5.2 Structural Prior Visualization

Before presenting the baseline comparison (Exp-2), we visualize the extracted Structural Importance Prior (SIP) that guides the high-dimensional layer-wise search.

Figure 3 summarizes, across Transformer layers, (i) L1-norm differences of task vectors, (ii) L2-norm differences, (iii) normalized differences used to produce importance scores, and (iv) the resulting lengthscale prior parameters used to initialize the SAAS-GP surrogate. The sensitivity is highly non-uniform across layers, motivating an importance-aware subspace Bayesian optimization strategy.

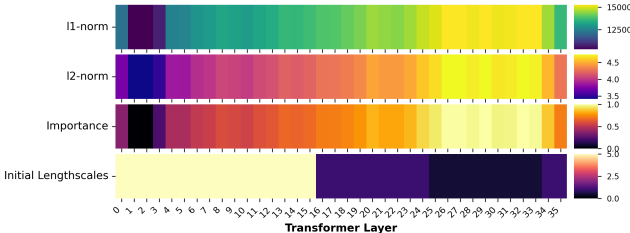


Figure 3: Visualization of the Structural Importance Prior (SIP) used in SIP-BMM. From top to bottom: task-vector L1 differences, L2 differences, normalized layer-wise differences (importance scores), and the mapped lengthscale priors for the SAAS-GP surrogate.

5.3 Main Results: SIP-BMM Vs. Baselines

Table 3 and Figure 4 present the performance of SIP-BMM compared to state-of-the-art model-level merging methods. SIP-BMM consistently discovers a stronger and denser Pareto front. While model-level baselines like task arithmetic and Breadcrumbs provide a few competitive points, they fail to explore the continuous spectrum of trade-offs.

Table 3: SIP-BMM against baseline merging methods (Summary).

METHOD	HV VALUE	COVERAGE	PARETO #
SIP-BMM (OURS)	1.397793	14/22	17
BREADCRUMBS	0.566634	1/22	2
TA	1.270630	3/22	13
DARE	1.257203	0/22	11
DELLA	1.301842	4/22	11
TIES	0.368805	0/22	5

SIP-BMM leverages the flexibility of layer-wise weights to find “sweet spots” where reasoning accuracy is maintained with significantly lower token counts. The hypervolume (HV) for SIP-BMM exceeds the best-performing baseline, demonstrating its effectiveness in navigating complex objective spaces.

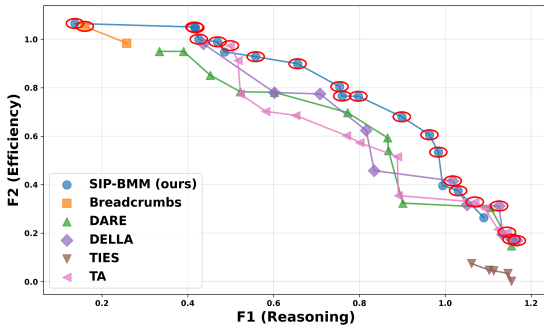


Figure 4: Distribution of merged models in objective space (f_1 vs. f_2).

To further understand performance on specific tasks, Figure 5 and Figure 6 show trade-offs between accuracy and token efficiency on each benchmark.

To further dissect the factors contributing to SIP-BMM’s performance, we study the impact of SIP through ablations.

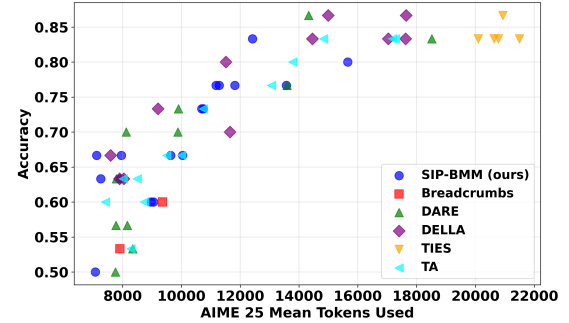


Figure 5: Pareto front on AIME25 (Tokens vs. Accuracy).

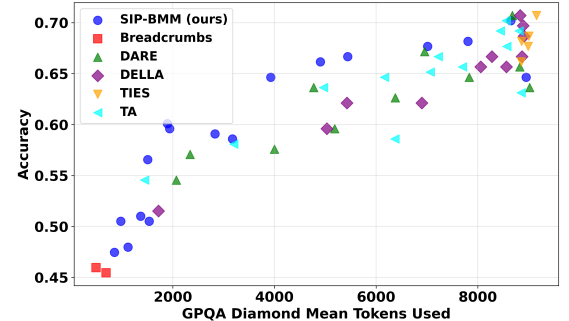


Figure 6: Pareto front on GPQA-Diamond (Tokens vs. Accuracy).

5.4 Ablation Study: Impact of SIP

We conduct an ablation study as shown in Figure 7.

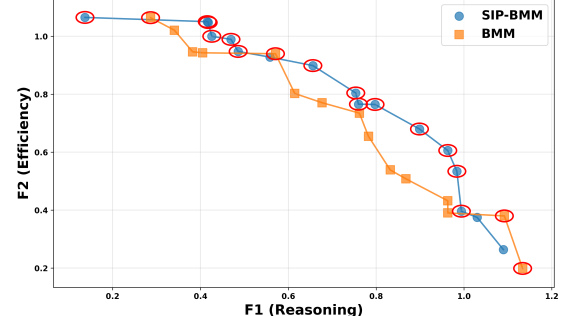


Figure 7: Ablation study results in objective space.

Table 5: Ablation study: Impact of SIP prior.

METHOD	HV VALUE	COVERAGE	PARETO #
SIP-BMM (OURS)	1.397793	14/18	17
SAAS-BO	1.358740	4/18	15

While vanilla SAASBO can eventually identify relevant dimensions, SIP-BMM achieves higher HV and coverage under the same evaluation budget. This indicates SIP provides an effective warm-start, allowing the sampler to focus on critical layers earlier. The results support that integrating architectural priors (SIP) with subspace optimization (SAASBO) is

Table 4: Detailed performance comparison of individual candidates across all methods.

ID	Method	f1 (↑)	f2 (↑)	GPQA_ACC (↑)	GPQA_TOKENS (↓)	AIME25_ACC (↑)	AIME25_TOKENS (↓)	Pareto
0	SIP-BMM (ours)	1.0301	0.3747	0.6465	8952	0.8334	12417	✓
1		0.4175	1.0474	0.4798	1116	0.6666	7120	✓
2		0.7597	0.7656	0.6465	3927	0.6667	10038	✓
3		0.6560	0.8988	0.5960	1937	0.6666	9638	✓
4		0.7976	0.7646	0.5859	3174	0.7667	11178	✓
5		0.4858	0.9476	0.5657	1503	0.6000	9053	✗
6		0.7537	0.8042	0.5909	2830	0.7333	10691	✓
7		0.9632	0.6057	0.6667	5440	0.7666	11815	✓
8		0.4155	1.0504	0.5051	973	0.6333	7256	✓
9		0.4695	0.9892	0.5051	1535	0.6666	7961	✓
10		0.5582	0.9280	0.6010	1894	0.6000	8968	✓
11		1.0898	0.2636	0.7020	8650	0.8000	15657	✗
12		0.1369	1.0650	0.4747	848	0.5000	7073	✓
13		0.9839	0.5339	0.6768	7015	0.7666	11286	✓
14		0.8987	0.6799	0.6616	4902	0.7333	10748	✓
15		0.4257	0.9999	0.5101	1368	0.6333	7939	✓
16		0.9942	0.3963	0.6818	7808	0.7666	13571	✗
0	Breadcrumbs	0.1599	1.0530	0.4596	490	0.5333	7906	✓
1		0.2576	0.9837	0.4545	686	0.6000	9357	✗
0–10	DARE	All candidates are non-Pareto in this run (dominated).						✗
1	DELLA (Pareto points)	1.0174	0.4153	0.6667	8872	0.8000	11517	✓
2		1.1255	0.3119	0.6667	8277	0.8667	14996	✓
4		1.1544	0.1745	0.7071	8834	0.8334	17624	✓
10		1.1670	0.1690	0.6869	8913	0.8667	17647	✓
0,3,5–9	DELLA (others)	Non-Pareto points omitted for brevity.						✗
0–4	TIES	All candidates are non-Pareto in this run (dominated).						✗
0	TA (Pareto points)	0.4983	0.9734	0.5455	1441	0.6333	8496	✓
9		1.0691	0.3285	0.6919	8812	0.8000	13786	✓
12		1.1438	0.2042	0.7020	8560	0.8333	17285	✓
1–8,10–11	TA (others)	Non-Pareto points omitted for brevity.						✗

crucial for sample-efficient LLM merging.

5.5 Solution Analysis

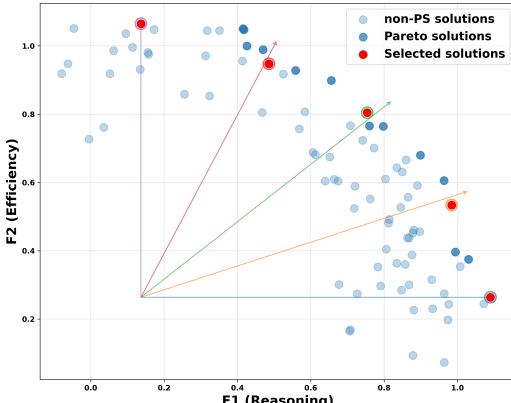


Figure 8: Visualization of Pareto-optimal and dominated solutions obtained by SIP-BMM.

Figure 8 visualizes the Pareto front and dominated solutions. Our framework supports rapid model customization based on user preferences: given a user-specified preference vector, we rank Pareto solutions by cosine similarity and select the best-matching model under the desired deployment constraints. To illustrate this customization capability without committing to a particular application scenario, we simulate user pref-

erences by sampling preference vectors from a uniform distribution over the trade-off space. As shown in the figure, the resulting Pareto set is both dense and diverse, providing good coverage across different capability–efficiency regimes and thus reliably satisfying heterogeneous preference distributions (including the uniformly distributed one used here) with minimal additional search. The detailed benchmark results for each selected model configuration are provided in the supplementary material.

6 Conclusion

We introduced SIP-BMM, a framework for constructing LLM Pareto sets by integrating Structural Importance Priors (SIP) with importance-aware SAASBO. We studied the fundamental trade-off between reasoning capability and efficiency, showing that coarse model-level merging is insufficient, while naive layer-wise optimization is hindered by the curse of dimensionality. By leveraging task-vector differences to quantify layer sensitivity, SIP-BMM identifies critical layers and guides the search within a sparse axis-aligned subspace, making fine-grained high-dimensional optimization feasible under strict evaluation budgets.

Experiments demonstrate that SIP-BMM outperforms competitive baselines, producing stronger and denser Pareto fronts with improved hypervolume. Our analysis confirms that combining architectural priors with subspace optimization bridges the gap between simplistic fusion and exhaustive search. SIP-BMM provides an automated pipeline for adaptive model selection, enabling deployment of LLMs tailored to evolving operational constraints.

Ethical Statement

There are no ethical issues.

References

[Akiba *et al.*, 2025] Takuya Akiba, Makoto Shing, Yujin Tang, Qi Sun, and David Ha. Evolutionary optimization of model merging recipes. *Nature Machine Intelligence*, 7(2):195–204, 2025.

[Daulton *et al.*, 2020] Samuel Daulton, Maximilian Balandat, and Eytan Bakshy. Differentiable expected hyper-volume improvement for parallel multi-objective bayesian optimization. *Advances in neural information processing systems*, 33:9851–9864, 2020.

[Daulton *et al.*, 2022] Samuel Daulton, Sait Cakmak, Maximilian Balandat, Michael A Osborne, Enlu Zhou, and Eytan Bakshy. Robust multi-objective bayesian optimization under input noise. In *International Conference on Machine Learning*, pages 4831–4866. PMLR, 2022.

[Davari and Belilovsky, 2024] MohammadReza Davari and Eugene Belilovsky. Model breadcrumbs: Scaling multi-task model merging with sparse masks. In *European Conference on Computer Vision*, pages 270–287. Springer, 2024.

[Deb *et al.*, 2002] Kalyanmoy Deb, Amrit Pratap, Sameer Agarwal, and TAMT Meyarivan. A fast and elitist multi-objective genetic algorithm: NSGA-II. *IEEE transactions on evolutionary computation*, 6(2):182–197, 2002.

[Deep *et al.*, 2024] Pala Tej Deep, Rishabh Bhardwaj, and Soujanya Poria. Della-merging: Reducing interference in model merging through magnitude-based sampling. *arXiv preprint arXiv:2406.11617*, 2024.

[Eriksson and Jankowiak, 2021] David Eriksson and Martin Jankowiak. High-dimensional bayesian optimization with sparse axis-aligned subspaces. In *Proceedings of the Thirty-Seventh Conference on Uncertainty in Artificial Intelligence*, pages 493–503. PMLR, 2021.

[Hansen *et al.*, 2003] Nikolaus Hansen, Sibylle D Müller, and Petros Koumoutsakos. Reducing the time complexity of the derandomized evolution strategy with covariance matrix adaptation (CMA-ES). *Evolutionary computation*, 11(1):1–18, 2003.

[Hoffman and Gelman, 2014] Matthew D Hoffman and Andrew Gelman. The No-U-Turn sampler: adaptively setting path lengths in hamiltonian monte carlo. *Journal of Machine Learning Research*, 15(1):1593–1623, 2014.

[Ilharco *et al.*, 2022] Gabriel Ilharco, Marco Túlio Ribeiro, Mitchell Wortsman, Suchin Gururangan, Ludwig Schmidt, Hannaneh Hajishirzi, and Ali Farhadi. Editing models with task arithmetic. *arXiv preprint arXiv:2212.04089*, 2022.

[Li *et al.*, 2025] Bingdong Li, Zixiang Di, Yanting Yang, Hong Qian, Peng Yang, Hao Hao, Ke Tang, and Aimin Zhou. It’s morphing time: Unleashing the potential of multiple llms via multi-objective optimization. *IEEE Transactions on Evolutionary Computation*, 2025.

[Rein *et al.*, 2024] David Rein, Betty Li Hou, Asa Cooper Stickland, Jackson Petty, Richard Yuanzhe Pang, Julien Dirani, Julian Michael, and Samuel R Bowman. Gpq: A graduate-level google-proof q&a benchmark. In *First Conference on Language Modeling*, 2024.

[Sui *et al.*, 2025] Yang Sui, Yu-Neng Chuang, Guanchu Wang, Jiamu Zhang, Tianyi Zhang, Jiayi Yuan, Hongyi Liu, Andrew Wen, Shaochen Zhong, Na Zou, et al. Stop overthinking: A survey on efficient reasoning for large language models. *arXiv preprint arXiv:2503.16419*, 2025.

[Team *et al.*, 2025] Kimi Team, Angang Du, Bofei Gao, Bowei Xing, Changjiu Jiang, Cheng Chen, Cheng Li, Chenjun Xiao, Chenzhuang Du, Chonghua Liao, et al. Kimi k1. 5: Scaling reinforcement learning with llms. *arXiv preprint arXiv:2501.12599*, 2025.

[Utans, 1996] Joachim Utans. Weight averaging for neural networks and local resampling schemes. In *Proc. AAAI-96 Workshop on Integrating Multiple Learned Models. AAAI Press*, pages 133–138. Citeseer, 1996.

[Wei *et al.*, 2022] Jason Wei, Xuezhi Wang, Dale Schuurmans, Maarten Bosma, Fei Xia, Ed Chi, Quoc V Le, Denny Zhou, et al. Chain-of-thought prompting elicits reasoning in large language models. *Advances in neural information processing systems*, 35:24824–24837, 2022.

[Williams and Rasmussen, 2006] Christopher KI Williams and Carl Edward Rasmussen. *Gaussian processes for machine learning*, volume 2. MIT press Cambridge, MA, 2006.

[Wu *et al.*, 2025] Taiqiang Wu, Runming Yang, Tao Liu, Jia-hao Wang, and Ngai Wong. Revisiting model interpolation for efficient reasoning. *arXiv preprint arXiv:2510.10977*, 2025.

[Yadav *et al.*, 2023] Prateek Yadav, Derek Tam, Leshem Choshen, Colin A Raffel, and Mohit Bansal. Ties-merging: Resolving interference when merging models. *Advances in Neural Information Processing Systems*, 36:7093–7115, 2023.

[Yang *et al.*, 2024] Enneng Yang, Li Shen, Guibing Guo, Xingwei Wang, Xiaochun Cao, Jie Zhang, and Dacheng Tao. Model merging in llms, mllms, and beyond: Methods, theories, applications and opportunities. *arXiv preprint arXiv:2408.07666*, 2024.

[Yang *et al.*, 2025] An Yang, Anfeng Li, Baosong Yang, Beichen Zhang, Binyuan Hui, Bo Zheng, Bowen Yu, Chang Gao, Chengan Huang, Chenxu Lv, et al. Qwen3 technical report. *arXiv preprint arXiv:2505.09388*, 2025.

[Yu *et al.*, 2024] Le Yu, Bowen Yu, Haiyang Yu, Fei Huang, and Yongbin Li. Language models are super mario: Absorbing abilities from homologous models as a free lunch. In *Forty-first International Conference on Machine Learning*, 2024.

A Analysis and Implementation of Block Partitioning

This appendix consolidates (i) the analysis of layer-wise task-vector differences and (ii) the formal implementation of the block partitioning strategy used for the granularity comparison in our experiments.

A.1 Layer-wise Difference Analysis and Visualization

Figure 9 visualizes the layer-wise ℓ_1 -norm and ℓ_2 -norm differences between the base model and expert models. We observe that the parameter differences are primarily concentrated in deeper layers, while shallow layers remain relatively stable. This aligns with the common understanding that deeper layers contribute more to high-level semantic processing (e.g., logical reasoning), whereas earlier layers capture more general, transferable features.

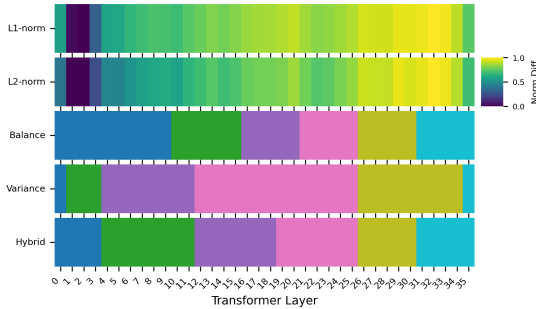


Figure 9: Visualization of layer-wise ℓ_1/ℓ_2 differences between task models and the resulting block partition strategies (Balance-only, Variance-only, and Hybrid).

A.2 Partitioning Strategies

Because layer-wise differences are non-uniform across depth, we compare three partitioning strategies:

- **Balance-only.** Enforces equal total difference per block. This often yields highly uneven block sizes (e.g., a single active deep layer forms a block, while many stable shallow layers are grouped together), which can distort the effective granularity of decision variables.
- **Variance-only.** Groups layers with similar difference magnitudes (e.g., Fisher–Jenks natural breaks), improving within-block homogeneity. However, it may result in blocks carrying very different amounts of “information mass”, creating imbalance across decision variables.
- **Hybrid strategy (ours).** Optimizes a trade-off between within-block homogeneity and across-block balance, typically isolating highly active deep layers into smaller, homogeneous blocks while keeping a reasonable distribution of total difference across blocks.

A.3 Formal Formulation and Dynamic Programming Algorithm

We cast layer partitioning as a variant of Fisher–Jenks natural breaks. Let $\{d_l\}_{l=1}^L$ denote a non-negative per-layer difference score computed from task vectors. We aim to partition

Algorithm 2 Hybrid Optimal Block Partitioning

```

1: Input: Task vectors  $\{TV_l^{(i)}\}$  for layers  $l = 1, \dots, L$ , number of blocks  $K$ , balance weight  $\lambda$ 
2: Output: Block partition  $\mathcal{P} = \{B_1, \dots, B_K\}$ 
3: Compute per-layer scores:
   
$$d_l \leftarrow \sum_{i=1}^N \left\| TV_l^{(i)} - \text{mean}(TV_l^{(i)}) \right\|_p$$

4: Target  $\leftarrow \left( \sum_{l=1}^L d_l \right) / K$ 
5: Precompute block costs for all  $1 \leq i \leq j \leq L$ :
   
$$\mathcal{C}(i, j) \leftarrow \text{Var}(d_{i:j}) \cdot (j - i + 1) + \lambda \cdot (\text{Sum}(d_{i:j}) - \text{Target})^2$$

6: Initialize  $\text{DP}[k][l] \leftarrow +\infty$ ; set  $\text{DP}[0][0] \leftarrow 0$ 
7: for  $k = 1$  to  $K$  do
8:   for  $l = 1$  to  $L$  do
9:     for  $m = k - 1$  to  $l - 1$  do
10:      if  $\text{DP}[k-1][m] + \mathcal{C}(m+1, l) < \text{DP}[k][l]$  then
11:         $\text{DP}[k][l] \leftarrow \text{DP}[k-1][m] + \mathcal{C}(m+1, l)$ 
12:         $\text{Split}[k][l] \leftarrow m$ 
13:      end if
14:    end for
15:  end for
16: end for
17: Reconstruct  $\mathcal{P}$  by backtracking  $\text{Split}[K][L]$ .

```

L layers into K contiguous blocks $\mathcal{P} = \{B_1, \dots, B_K\}$ that minimize a hybrid objective:

$$\min_{\mathcal{P}} J(\mathcal{P}) = \sum_{k=1}^K \text{Cost}(B_k) = \sum_{k=1}^K (\text{Var}(B_k) + \lambda \cdot \text{Dev}(B_k)), \quad (11)$$

where $\text{Var}(B_k)$ is the within-block variance and $\text{Dev}(B_k)$ penalizes deviation from a target block sum:

$$\text{Var}(B_k) = \sum_{l \in B_k} (d_l - \mu_{B_k})^2, \quad (12)$$

$$\text{Dev}(B_k) = \left(\sum_{l \in B_k} d_l - \text{Target} \right)^2, \quad (13)$$

$$\text{Target} = \frac{\sum_{l=1}^L d_l}{K}. \quad (14)$$

Here, μ_{B_k} denotes the mean of $\{d_l : l \in B_k\}$, and $\lambda \geq 0$ controls the balance–homogeneity trade-off.

We solve this optimization via dynamic programming (DP). Define $\mathcal{C}(i, j)$ as the cost of forming a block containing contiguous layers i, \dots, j . Then:

$$\text{DP}[k][l] = \min_{m \in \{k-1, \dots, l-1\}} \{\text{DP}[k-1][m] + \mathcal{C}(m+1, l)\}, \quad (15)$$

with $\text{DP}[0][0] = 0$ and $\text{DP}[0][l > 0] = +\infty$. The optimal partition is recovered by backtracking the split points.

A.4 Proof of Optimality

Theorem 1. Let $\text{DP}[k][l]$ be defined by the recurrence

$$\text{DP}[k][l] = \min_m \{\text{DP}[k-1][m] + \mathcal{C}(m+1, l)\},$$

with standard base cases. Then $\text{DP}[K][L]$ equals the globally minimum cost for partitioning L layers into K contiguous blocks under the additive objective $\sum_{k=1}^K \text{Cost}(B_k)$.

Proof. We prove by induction on k . For $k = 1$, there is only one feasible partition: a single block covering all layers $1:l$, and the DP value matches this cost. Assume for $k - 1$ that $\text{DP}[k-1][m]$ equals the minimum cost among all partitions of the first m layers into $k - 1$ blocks. For k blocks partitioning the first l layers, any feasible solution must end with some final block $(m+1):l$, preceded by a valid partition of $1:m$ into $k - 1$ blocks. By the inductive hypothesis, the minimum achievable cost of the prefix is $\text{DP}[k-1][m]$, hence the total cost is at least $\text{DP}[k-1][m] + \mathcal{C}(m+1, l)$. Taking the minimum over all valid split points m yields exactly the global optimum, which is the DP recurrence. Therefore, $\text{DP}[K][L]$ is globally optimal. \square

B Detailed Baseline Formulations

This appendix provides the mathematical definitions for model-level merging baselines used in our experiments. Let $\mathcal{M}^{(\text{base})}$ be the base model and $\mathcal{M}^{(i)}$ the i -th expert model. Define the task vector

$$TV^{(i)} := \mathcal{M}^{(i)} - \mathcal{M}^{(\text{base})}.$$

B.1 Task Arithmetic

Task Arithmetic steers the base model by adding a weighted sum of task vectors:

$$\mathcal{M}^{(\text{merge})} = \mathcal{M}^{(\text{base})} + \alpha \sum_{i=1}^T TV^{(i)}. \quad (16)$$

B.2 TIES-Merging

TIES addresses parameter conflicts using sparsification, sign resolution, and selective merging. A simplified form can be written as:

$$\mathcal{M}^{(\text{merge})} = \mathcal{M}^{(0)} + \alpha \cdot \text{top-k}\left(TV^{(i)}\right), \quad (17)$$

where $\text{top-k}(\cdot)$ keeps the largest-magnitude parameters.

B.3 DARE-Merging

DARE (Drop And REscale) randomly drops a fraction p of delta parameters and rescales the rest:

$$\mathcal{M}^{(\text{merge})} = \mathcal{M}^{(\text{base})} + \alpha \sum_{i=1}^T \text{DARE}\left(TV^{(i)}, p\right). \quad (18)$$

B.4 Breadcrumbs

Breadcrumbs applies sparsification and masking to remove both large outliers and small perturbations:

$$\mathcal{M}^{(\text{merge})} = \mathcal{M}^{(\text{base})} + \alpha \sum_{i=1}^T m^{(i)} \odot TV^{(i)}, \quad (19)$$

where $m^{(i)}$ is a mask and \odot denotes element-wise multiplication.

B.5 DELLA

DELLA (Drop–Elect–Fuse) drops parameters, elects deltas with consistent signs, and fuses them:

$$\mathcal{M}^{(\text{merge})} = \mathcal{M}^{(\text{base})} + \lambda \cdot \delta^{(\text{avg})}, \quad (20)$$

where $\delta^{(\text{avg})}$ is the averaged and rescaled delta after the Drop–Elect–Fuse pipeline.

C Detailed Experimental Results

Table 8 reports the complete set of evaluated configurations across different merging granularities.

D Surrogate Model and Kernel Specifications

D.1 ARD Matérn-5/2 Kernel

To model the non-linear landscape of LLM merging, we use the Matérn-5/2 kernel with Automatic Relevance Determination (ARD). For two configurations $\mathbf{x}, \mathbf{x}' \in [0, 1]^D$, the kernel is:

$$k(\mathbf{x}, \mathbf{x}') = \sigma_f^2 \left(1 + \sqrt{5}r + \frac{5}{3}r^2 \right) \exp(-\sqrt{5}r), \quad (21)$$

where

$$r(\mathbf{x}, \mathbf{x}') = \sqrt{\sum_{d=1}^D \frac{(x_d - x'_d)^2}{\ell_d^2}}. \quad (22)$$

D.2 Hierarchical SAAS Prior for Sparsity

In high-dimensional LLM merging, most layers may have negligible impact on the resulting Pareto frontier. Following [Eriksson and Jankowiak, 2021], we place a Sparse Axis-Aligned Subspace (SAAS) prior on the inverse squared lengthscales $\rho_d = 1/\ell_d^2$:

$$\tau \sim \text{Half-Cauchy}(0.1), \quad \rho_d \sim \text{Half-Cauchy}(\tau), \quad d = 1, \dots, D. \quad (23)$$

Here τ is a global shrinkage parameter encouraging most ρ_d to be near zero (i.e., $\ell_d \rightarrow \infty$), effectively pruning irrelevant dimensions; only a few critical dimensions with large ρ_d remain active.

D.3 Fully Bayesian Inference via NUTS

Unlike standard Bayesian optimization that often uses MLE/MAP for hyperparameter fitting, SIP-BMM uses fully Bayesian inference to account for hyperparameter uncertainty, which is particularly important when the evaluation budget is small. Let $\theta = \{\rho_{1:D}, \sigma_f^2, \sigma_e^2\}$ denote GP hyperparameters. We infer:

$$p(\theta | \mathcal{D}) \propto p(\mathcal{Y} | \mathcal{X}, \theta) p(\theta), \quad (24)$$

and draw samples $\{\theta^{(m)}\}_{m=1}^M$ using the No-U-Turn Sampler (NUTS). The acquisition function is integrated over hyperparameter samples:

$$\alpha(\mathbf{x}) = \frac{1}{M} \sum_{m=1}^M \alpha(\mathbf{x}; \theta^{(m)}). \quad (25)$$

D.4 SIP-Guided Warm-Start for NUTS Initialization

The efficiency of NUTS in high dimensions depends on chain initialization. We use the Structural Importance Prior (SIP) to warm-start the initial lengthscales by setting ℓ_d to SIP-derived values $\ell_d^{(0)}$ (as defined in the main paper). Since the kernel sensitivity to dimension d scales as $|\partial k / \partial x_d| \propto 1/\ell_d^2$, initializing critical layers with smaller $\ell_d^{(0)}$ (e.g., 0.5) biases early sampling toward functionally active dimensions, while stable layers can be initialized with larger values (e.g., 5.0). This enables SIP-BMM to approach the Pareto frontier more quickly than vanilla SAASBO under limited evaluations.

E qNEHVI Implementation Details

Attribution. We use the q NEHVI acquisition and the corresponding log-stabilized Monte-Carlo estimator from [Daulton *et al.*, 2022].

Decision space and objective vector (same as main text). Our decision variable is the layer-wise merging vector $\mathbf{x} \in [0, 1]^D$ with $D = L$,

$$\mathbf{x} = (x_1, \dots, x_L), \quad x_l \in [0, 1], \quad l = 1, \dots, L. \quad (26)$$

Each \mathbf{x} defines a merged model $\mathcal{M}_{\text{merge}}(\mathbf{x}) = \text{Layer-Wise-Merge}(\{\mathcal{M}_i\}; \mathbf{x})$, which is evaluated by the K normalized objectives $y_k(\mathbf{x}) := f_k(\mathcal{M}_{\text{merge}}(\mathbf{x}))$. We collect them into the objective vector

$$\mathbf{y}(\mathbf{x}) = (y_1(\mathbf{x}), \dots, y_K(\mathbf{x})) = (f_1(\mathcal{M}_{\text{merge}}(\mathbf{x})), \dots, f_K(\mathcal{M}_{\text{merge}}(\mathbf{x}))) \in \mathbb{R}^K. \quad (27)$$

All objectives are maximized in this normalized space.

Data at iteration t and observed nondominated set. At BO iteration t , we have the evaluation dataset $\mathcal{D}_t = \{(\mathbf{x}_i, \mathbf{y}_i)\}_{i=1}^{n_t}$ with $\mathbf{y}_i = \mathbf{y}(\mathbf{x}_i)$. Let

$$\mathcal{P}_t \subseteq \{\mathbf{y}_i\}_{i=1}^{n_t} \quad (28)$$

denote the set of *observed* nondominated objective vectors (Pareto set in objective space). Let $\mathbf{r} \in \mathbb{R}^K$ be a fixed reference point.

Hypervolume improvement (HVI). Given q new objective vectors $\mathbf{Y} = \{\mathbf{y}^{(1)}, \dots, \mathbf{y}^{(q)}\}$, the deterministic hypervolume improvement is

$$\text{HVI}(\mathbf{Y}; \mathcal{P}_t, \mathbf{r}) = \text{HV}(\mathcal{P}_t \cup \mathbf{Y}; \mathbf{r}) - \text{HV}(\mathcal{P}_t; \mathbf{r}), \quad (29)$$

where $\text{HV}(\cdot; \mathbf{r})$ is the dominated hypervolume w.r.t. \mathbf{r} .

Noisy Pareto samples $\tilde{\mathcal{P}}_t$ (accounting for observation noise). We fit a multi-objective surrogate at iteration t as K independent SAAS GPs to model each scalar objective $y_k(\mathbf{x})$. In the noisy EHVI setting, the nondominated set used in HVI is treated as random: $\tilde{\mathcal{P}}_t$ is formed by sampling latent (noise-free) outcomes of the already-evaluated points from the GP posterior and taking the nondominated subset [Daulton *et al.*, 2022]. Concretely, for each Monte-Carlo draw $n = 1, \dots, N$ we sample

$$\tilde{\mathbf{y}}_i^{(n)} \sim p(\mathbf{y}(\mathbf{x}_i) \mid \mathcal{D}_t), \quad i = 1, \dots, n_t, \quad (30)$$

and define

$$\tilde{\mathcal{P}}_t^{(n)} := \text{ND}\left(\{\tilde{\mathbf{y}}_i^{(n)}\}_{i=1}^{n_t}\right), \quad (31)$$

where $\text{ND}(\cdot)$ returns the nondominated subset under Pareto dominance (maximization).

q NEHVI acquisition for a batch of merge vectors. We optimize a batch of q candidate merge vectors $\mathbf{X} = \{\mathbf{x}^{(i)}\}_{i=1}^q \subset [0, 1]^D$. This batch induces random objective vectors under the GP posterior:

$$\mathbf{Y}(\mathbf{X}) = \{\mathbf{y}(\mathbf{x}^{(i)})\}_{i=1}^q. \quad (32)$$

The q NEHVI acquisition is the posterior expectation

$$\alpha_{q\text{NEHVI}}(\mathbf{X}) = \mathbb{E}_{\tilde{\mathcal{P}}_t, \mathbf{Y}(\mathbf{X}) \mid \mathcal{D}_t} [\text{HVI}(\mathbf{Y}(\mathbf{X}); \tilde{\mathcal{P}}_t, \mathbf{r})], \quad (33)$$

Monte-Carlo estimator and log-stabilized evaluation. We approximate Eq. (33) with Monte-Carlo samples from the *joint* posterior of the batch outcomes:

$$\hat{\alpha}_{q\text{NEHVI}}^{(N)}(\mathbf{X}) = \frac{1}{N} \sum_{n=1}^N \text{HVI}\left(\mathbf{Y}^{(n)}(\mathbf{X}); \tilde{\mathcal{P}}_t^{(n)}, \mathbf{r}\right), \quad (34)$$

where $\mathbf{Y}^{(n)}(\mathbf{X})$ is the n -th posterior draw of $\mathbf{Y}(\mathbf{X})$ and $\tilde{\mathcal{P}}_t^{(n)}$ is the corresponding noisy Pareto sample defined above. Following [Daulton *et al.*, 2022], we compute the MC objective using a log-stabilized formulation of the improvement term to avoid numerical underflow/overflow when improvements become very small (common near convergence), while the underlying utility remains (noisy) expected hypervolume improvement.

Table 6: Detailed individual metrics for different merging granularities (full data).

ID	Method	f1 (↑)	f2 (↑)	GPQA_ACC (↑)	GPQA_TOKENS (↓)	AIME25_ACC (↑)	AIME25_TOKENS (↓)	Pareto
0	Layer-wise	0.8698	0.8047	0.6212	4037	0.7666	8891	✓
1		0.9527	0.2414	0.6616	9136	0.7666	15496	✗
2		0.3656	1.0585	0.4545	791	0.6666	7321	✓
3		0.6848	0.8697	0.6364	3427	0.6333	8161	✓
4		0.3428	1.0599	0.4697	958	0.6333	7037	✓
5		0.1783	1.0666	0.4949	764	0.5000	7158	✓
6		0.2116	1.0600	0.4848	717	0.5333	7392	✓
7		0.8826	0.7393	0.6010	4308	0.8000	10132	✓
8		0.5753	1.0409	0.5303	900	0.7000	7602	✓
9		0.6101	0.9011	0.6263	2509	0.6000	8732	✓
0	Block-wise (n=18)	1.0691	0.5632	0.6919	6660	0.8000	11077	✓
1		0.6894	0.7855	0.5859	4706	0.7000	8384	✗
2		0.5086	1.0210	0.5505	1573	0.6333	7106	✗
3		0.7308	0.7012	0.6061	5104	0.7000	9912	✗
4		0.1266	1.0383	0.4697	981	0.5000	7545	✗
5		0.5455	0.9135	0.6212	2698	0.5666	8140	✗
6		0.8677	0.6257	0.6465	6076	0.7333	10369	✗
7		0.7183	0.7383	0.6263	3923	0.6667	10729	✗
8		0.8552	0.6671	0.6667	5376	0.7000	10366	✗
0	Block-wise (n=9)	0.9320	0.4935	0.6515	7576	0.7666	11472	✗
1		0.9735	0.3001	0.6717	8549	0.7666	14888	✗
2		0.8552	0.5161	0.6667	7219	0.7000	11430	✗
3		0.7411	0.6215	0.6111	6391	0.7000	10008	✗
4		0.5628	0.8946	0.5505	1273	0.6667	10726	✗
5		0.6284	0.8021	0.6616	4832	0.5666	7779	✗
6		0.4776	0.9933	0.5354	1680	0.6333	7643	✗
7		1.0611	0.2645	0.6616	8242	0.8334	16240	✗
8		0.7930	0.6184	0.6364	6471	0.7000	9968	✗
9	Model-level	1.0818	0.2037	0.6717	8082	0.8334	18005	✗
10		0.3822	1.0249	0.5152	1226	0.6000	7520	✗
11		1.0715	0.2445	0.6667	8176	0.8334	16841	✗
12		1.0506	0.2790	0.6566	8406	0.8333	15631	✗
13		0.9506	0.3431	0.6869	8263	0.7333	14233	✗
0		0.4983	0.9734	0.5455	1441	0.6333	8496	✗
1		0.5168	0.9129	0.5808	3197	0.6000	7417	✗
2		0.5227	0.7743	0.6364	4966	0.5333	8279	✗
3		0.6516	0.6855	0.6465	6165	0.6000	8735	✗
4		0.5812	0.7023	0.5859	6368	0.6333	8013	✗
5		0.7700	0.6019	0.6515	7065	0.6667	9503	✗
6		0.8012	0.5726	0.6667	7220	0.6667	10008	✗
7		0.8885	0.5154	0.6566	7697	0.7333	10740	✗
8		0.8906	0.3548	0.6313	8851	0.7666	13067	✗
9	AIME25	1.0691	0.3285	0.6919	8812	0.8000	13786	✗
10		1.0923	0.3010	0.6768	8571	0.8334	14834	✓
11		1.1231	0.2153	0.6919	8443	0.8333	17178	✓
12		1.1438	0.2042	0.7020	8560	0.8333	17285	✓

Evaluation Results for Selected LLM Pareto Solutions

Table 7: Evaluation Results for Selected LLM Pareto Solutions

Solution ID	Content
1	<p>Question: Answer the following multiple choice question. The last line of your response should be of the following format: 'ANSWER: \$LETTER' (without quotes) where LETTER is one of A,B,C,D. Think step by step before answering.</p> <p>Two quantum states with energies E_1 and E_2 have a lifetime of 10^{-9} sec and 10^{-8} sec, respectively. We want to clearly distinguish these two energy levels. Which one of the following options could be their energy difference so that they can be clearly resolved?</p> <p>Options: A) 10^{-9} eV B) 10^{-8} eV C) 10^{-4} eV D) 10^{-11} eV</p> <p>Model Answer: C Correct Answer: C Character Count: 454.0</p> <p>Full Answer: To determine the energy difference that allows clear resolution between two quantum states, we need to consider the energy uncertainty principle, which relates the energy of a state to its lifetime. The energy-time uncertainty principle states that: $\Delta E \cdot \Delta t \geq \frac{\hbar}{2}$ where: - ΔE is the energy uncertainty (related to the energy difference we want to resolve) - Δt is the lifetime of the state - \hbar is the reduced Planck's constant ($\approx 6.582 \times 10^{-16}$ eV·s)</p> <p>For a state with lifetime Δt, the energy uncertainty is approximately: $\Delta E \approx \hbar/\Delta t$</p> <p>So for each state: For E_1 with $\Delta t = 10^{-9}$ sec: $\Delta E_1 \approx (6.582 \times 10^{-16} \text{ eV}\cdot\text{s}) / (10^{-9} \text{ s}) = 6.582 \times 10^{-7} \text{ eV} \approx 10^{-6} \text{ eV}$</p> <p>For E_2 with $\Delta t = 10^{-8}$ sec: $\Delta E_2 \approx (6.582 \times 10^{-16} \text{ eV}\cdot\text{s}) / (10^{-8} \text{ s}) = 6.582 \times 10^{-8} \text{ eV} \approx 10^{-7} \text{ eV}$</p> <p>The energy difference between the two states must be larger than the energy uncertainty of each state to be resolved. So we need an energy difference larger than both ΔE_1 and ΔE_2.</p> <p>Looking at the options: A) 10^{-9} eV (too small) B) 10^{-8} eV (smaller than ΔE_2) C) 10^{-4} eV (larger than both ΔE_1 and ΔE_2) D) 10^{-11} eV (too small)</p> <p>Option C (10^{-4} eV) is the only one that is larger than both energy uncertainties and thus can be clearly resolved.</p> <p>ANSWER: C</p>
2	<p>Question: Answer the following multiple choice question. The last line of your response should be of the following format: 'ANSWER: \$LETTER' (without quotes) where LETTER is one of A,B,C,D. Think step by step before answering.</p> <p>Two quantum states with energies E_1 and E_2 have a lifetime of 10^{-9} sec and 10^{-8} sec, respectively. We want to clearly distinguish these two energy levels. Which one of the following options could be their energy difference so that they can be clearly resolved?</p> <p>Options: A) 10^{-9} eV B) 10^{-8} eV C) 10^{-4} eV D) 10^{-11} eV</p> <p>Model Answer: C Correct Answer: C Character Count: 457.0</p> <p>Full Answer: To determine which energy difference allows us to clearly distinguish the two quantum states, we need to consider the uncertainty principle, specifically the energy-time uncertainty relation: $\Delta E \cdot \Delta t \geq \frac{\hbar}{2}$ Where: - ΔE is the energy uncertainty - Δt is the lifetime of the state - \hbar is the reduced Planck constant ($\approx 6.58 \times 10^{-16}$ eV·s)</p> <p>For a state with lifetime Δt, the energy uncertainty ΔE is approximately $\hbar/\Delta t$.</p> <p>Let's calculate the energy uncertainty for each lifetime:</p> <p>For $\Delta t = 10^{-9}$ sec: $\Delta E \approx \frac{6.58 \times 10^{-16} \text{ eV}\cdot\text{s}}{10^{-9} \text{ s}} = 6.58 \times 10^{-7} \text{ eV}$</p> <p>For $\Delta t = 10^{-8}$ sec: $\Delta E \approx \frac{6.58 \times 10^{-16} \text{ eV}\cdot\text{s}}{10^{-8} \text{ s}} = 6.58 \times 10^{-8} \text{ eV}$</p> <p>The energy difference between the two states must be larger than the energy uncertainty of the shorter-lived state (since it has the larger uncertainty) to be clearly resolved. The shorter-lived state has a larger energy uncertainty (10^{-9} sec has larger uncertainty than 10^{-8} sec).</p> <p>So the energy difference should be larger than the larger of these two uncertainties ($6.58 \times 10^{-8} \text{ eV} \approx 10^{-7} \text{ eV}$).</p> <p>Looking at the options: A) 10^{-9} eV (too small) B) 10^{-8} eV (smaller than 10^{-7} eV, so not clearly resolved) C) 10^{-4} eV (larger than 10^{-7} eV, so it could be resolved) D) 10^{-11} eV (too small)</p> <p>Option C (10^{-4} eV) is the only one that is larger than the energy uncertainty of the shorter-lived state (10^{-7} eV), so it would allow clear distinction.</p> <p>ANSWER: C</p>

Continued on next page

Table 7 – *Continued from previous page*

ID	Content
3	<p>Question: Answer the following multiple choice question. The last line of your response should be of the following format: 'ANSWER: \$LETTER' (without quotes) where LETTER is one of A,B,C,D. Think step by step before answering.</p> <p>Two quantum states with energies E_1 and E_2 have a lifetime of 10^{-9} sec and 10^{-8} sec, respectively. We want to clearly distinguish these two energy levels. Which one of the following options could be their energy difference so that they can be clearly resolved?</p> <p>Options: A) 10^{-9} eV B) 10^{-8} eV C) 10^{-4} eV D) 10^{-11} eV</p> <p>Model Answer: C Correct Answer: C Character Count: 459.0</p> <p>Full Answer: To determine which energy difference would allow us to clearly distinguish the two energy levels, I need to consider the uncertainty principle. The energy-time uncertainty principle states that $\Delta E \cdot \Delta t \geq \hbar/2$, where ΔE is the energy uncertainty and Δt is the lifetime of the state.</p> <p>For each state: - State 1 has a lifetime of 10^{-9} sec, so $\Delta E_1 \approx \hbar/(2 \times 10^{-9})$ - State 2 has a lifetime of 10^{-8} sec, so $\Delta E_2 \approx \hbar/(2 \times 10^{-8})$</p> <p>The energy difference ΔE between the two states must be larger than the individual energy uncertainties to be clearly resolved. So we need $\Delta E > \max(\Delta E_1, \Delta E_2)$.</p> <p>Let's calculate the energy uncertainties approximately: - $\hbar \approx 6.582 \times 10^{-16}$ eV·s - $\Delta E_1 \approx 6.582 \times 10^{-16}/(2 \times 10^{-9}) \approx 3.29 \times 10^{-7}$ eV - $\Delta E_2 \approx 6.582 \times 10^{-16}/(2 \times 10^{-8}) \approx 3.29 \times 10^{-8}$ eV</p> <p>So the larger uncertainty is $\Delta E_1 \approx 3.29 \times 10^{-7}$ eV. Therefore, the energy difference must be larger than this value to be clearly resolved.</p> <p>Looking at the options: A) 10^{-9} eV - too small B) 10^{-8} eV - still smaller than 3.29×10^{-7} eV C) 10^{-4} eV - larger than 3.29×10^{-7} eV D) 10^{-11} eV - too small</p> <p>Option C is the only one that is larger than the larger energy uncertainty (3.29×10^{-7} eV), so it would allow clear resolution of the two energy levels.</p> <p>ANSWER: C</p>
4	<p>Question: Answer the following multiple choice question. The last line of your response should be of the following format: 'ANSWER: \$LETTER' (without quotes) where LETTER is one of A,B,C,D. Think step by step before answering.</p> <p>Two quantum states with energies E_1 and E_2 have a lifetime of 10^{-9} sec and 10^{-8} sec, respectively. We want to clearly distinguish these two energy levels. Which one of the following options could be their energy difference so that they can be clearly resolved?</p> <p>Options: A) 10^{-9} eV B) 10^{-8} eV C) 10^{-4} eV D) 10^{-11} eV</p> <p>Model Answer: C Correct Answer: C Character Count: 2983.0</p> <p>Full Answer: First, I need to recall the relationship between the lifetime of a quantum state and the energy uncertainty. This comes from the Heisenberg uncertainty principle, which states that the product of the uncertainty in energy (ΔE) and the uncertainty in time (Δt) is approximately $\hbar/2$. For a state with a lifetime τ, the energy uncertainty is roughly $\Delta E \approx \hbar/\tau$.</p> <p>The uncertainty principle is $\Delta E \cdot \Delta t \geq \hbar/2$. For a state with lifetime τ, we often take $\Delta t \approx \tau$, so $\Delta E \approx \hbar/(2\tau)$. But for rough estimates, we can say $\Delta E \approx \hbar/\tau$.</p> <p>Now, \hbar is the reduced Planck's constant. I remember that $\hbar = h/(2\pi)$, and h is about $4.135667662 \times 10^{-15}$ eV·s (I think it's better to use a standard value). I know that $\hbar c$ is often used in particle physics, but for energy, let's think in eV and seconds.</p> <p>A common approximation is that $\hbar \approx 6.582 \times 10^{-16}$ eV·s. Let me confirm that.</p> <p>Yes, $\hbar = h/(2\pi) \approx (4.135667662 \times 10^{-15})/(2\pi) \approx 6.582 \times 10^{-16}$ eV·s. That sounds right.</p> <p>So, $\Delta E \approx \hbar/\tau$.</p> <p>Now, the problem gives lifetimes: $\tau_1 = 10^{-9}$ sec for E_1, $\tau_2 = 10^{-8}$ sec for E_2.</p> <p>We want to clearly distinguish these two energy levels. That means the energy difference between them should be larger than the energy uncertainty of each state.</p> <p>To resolve two energy levels, the energy difference ΔE should be greater than the larger of the two energy uncertainties, because if it's smaller than both, they might not be distinguishable.</p> <p>The uncertainty for E_1 is $\Delta E_1 \approx \hbar/\tau_1$, and for E_2 is $\Delta E_2 \approx \hbar/\tau_2$.</p> <p>Since $\tau_1 = 10^{-9}$ s and $\tau_2 = 10^{-8}$ s, τ_1 is smaller than τ_2, so ΔE_1 should be larger than ΔE_2 because ΔE is inversely proportional to τ.</p>

Continued on next page

Table 7 – *Continued from previous page*

ID	Content
4	<p>Let me calculate the uncertainties.</p> <p>First, for E_1: $\tau_1 = 1.0 \times 10^{-9}$ s $\Delta E_1 \approx \hbar/\tau_1 \approx (6.582 \times 10^{-16} \text{ eV}\cdot\text{s})/(1.0 \times 10^{-9} \text{ s}) = 6.582 \times 10^{-7} \text{ eV}$</p> <p>Similarly, for E_2: $\tau_2 = 1.0 \times 10^{-8}$ s $\Delta E_2 \approx \hbar/\tau_2 \approx (6.582 \times 10^{-16} \text{ eV}\cdot\text{s})/(1.0 \times 10^{-8} \text{ s}) = 6.582 \times 10^{-8} \text{ eV}$</p> <p>So, $\Delta E_1 \approx 6.6 \times 10^{-7} \text{ eV}$ and $\Delta E_2 \approx 6.6 \times 10^{-8} \text{ eV}$.</p> <p>The larger uncertainty is $\Delta E_1 \approx 10^{-6.18} \text{ eV}$, which is about $6.6 \times 10^{-7} \text{ eV}$, so roughly 10^{-6} eV.</p> <p>To clearly distinguish the two energy levels, the energy difference ΔE between them should be larger than the larger uncertainty, which is $\Delta E_1 \approx 10^{-6} \text{ eV}$.</p> <p>Now, looking at the options:</p> <p>A) 10^{-9} eV B) 10^{-8} eV C) 10^{-4} eV D) 10^{-11} eV 10^{-4} eV is 0.0001 eV, which is larger than 10^{-6} eV (0.000001 eV). 10^{-4} is 100 times larger than 10^{-6}.</p> <p>10^{-9} eV is smaller than 10^{-6} eV, 10^{-8} is also smaller, 10^{-11} is much smaller.</p> <p>So, only option C, 10^{-4} eV, is larger than the larger uncertainty $\Delta E_1 \approx 10^{-6} \text{ eV}$.</p> <p>I should double-check the uncertainty calculation.</p> <p>Sometimes the uncertainty is given as $\Delta E = \hbar/(2\tau)$, but for comparison purposes, the factor of 2 doesn't change the order of magnitude.</p> <p>Let me calculate numerically.</p> <p>$\hbar = 1.0545718 \times 10^{-34} \text{ J}\cdot\text{s}$</p> <p>But we need eV.</p> <p>$1 \text{ eV} = 1.60217662 \times 10^{-19} \text{ J}$</p> <p>So \hbar in $\text{eV}\cdot\text{s} = (1.0545718 \times 10^{-34})/(1.60217662 \times 10^{-19}) \approx 6.582 \times 10^{-16} \text{ eV}\cdot\text{s}$, as I had.</p> <p>$\tau_1 = 10^{-9} \text{ s}$ $\Delta E_1 = \hbar/\tau_1 = 6.582 \times 10^{-16}/1 \times 10^{-9} = 6.582 \times 10^{-7} \text{ eV} \approx 6.6 \times 10^{-7} \text{ eV}$</p> <p>Similarly, $\Delta E_2 = 6.582 \times 10^{-16}/1 \times 10^{-8} = 6.582 \times 10^{-8} \text{ eV} \approx 6.6 \times 10^{-8} \text{ eV}$</p> <p>So the energy difference needs to be greater than about 10^{-6} eV to be resolved from the uncertainty of the first state.</p> <p>Option C is 10^{-4} eV, which is 0.0001 eV, while 10^{-6} is 0.000001, so 10^{-4} is 100 times larger, so yes, it should be resolvable.</p> <p>Option A is 10^{-9}, which is 0.000000001, much smaller than 10^{-6}.</p> <p>B is 10^{-8}, still smaller than 10^{-6}.</p> <p>D is 10^{-11}, even smaller.</p> <p>So only C is larger than the uncertainty.</p> <p>The question says "clearly distinguish these two energy levels". In spectroscopy, to resolve two lines, the energy difference should be larger than the natural width of the lines.</p> <p>The natural width $\Gamma = \hbar/\tau$ for each state.</p> <p>So for E_1, $\Gamma_1 = \hbar/\tau_1$, for E_2, $\Gamma_2 = \hbar/\tau_2$.</p> <p>The minimum energy difference to resolve them is roughly the larger of Γ_1 and Γ_2, since if $\Delta E < \Gamma_1$, they might overlap.</p> <p>In this case, $\Gamma_1 > \Gamma_2$, so $\Delta E > \Gamma_1 \approx 10^{-6} \text{ eV}$.</p> <p>Option C is 10^{-4} eV, which is larger.</p> <p>I recall that in some contexts, for two states to be resolved, ΔE should be greater than the average or something, but I think the standard is that it should be larger than the energy uncertainty of the state with the shorter lifetime, since it has the broader line.</p> <p>Yes, because the state with shorter lifetime has larger uncertainty, so it's harder to resolve if the energy difference is small.</p> <p>So, for E_1 with $\tau = 10^{-9} \text{ s}$, Γ_1 is larger, so ΔE must be $> \Gamma_1$.</p> <p>$\Gamma_1 \approx 6.6 \times 10^{-7} \text{ eV}$, so 10^{-4} eV is 100 times larger, so it should be clear.</p> <p>Let me see the options again. Option C is 10^{-4} eV.</p> <p>Is there a trick? The lifetimes are given, but the energy difference is what we're to choose.</p> <p>Another way: the energy difference should be much larger than the uncertainties.</p> <p>The question says "could be their energy difference so that they can be clearly resolved".</p> <p>So, among the options, which one is larger than the larger uncertainty.</p> <p>Larger uncertainty is $\Gamma_1 \approx 10^{-6} \text{ eV}$ (since 6.6×10^{-7} is about $10^{-6.2}$, so roughly 10^{-6}).</p> <p>10^{-4} is 100 times larger, so yes.</p> <p>10^{-8} is smaller than 10^{-6}, so it wouldn't be resolved.</p> <p>For example, if $\Delta E = 10^{-8} \text{ eV}$, and $\Gamma_1 = 10^{-6} \text{ eV}$, then $\Delta E < \Gamma_1$, so the lines would overlap significantly.</p>

Continued on next page

Table 7 – *Continued from previous page*

ID	Content
	<p>Similarly, for $\Delta E = 10^{-4}$ eV, it's much larger, so they can be resolved. I think C is correct. But let me see why the other options might be tempting. Option D is 10^{-11} eV, which is tiny. Option A and B are smaller. Perhaps someone might think that the energy difference should be related to the difference in lifetimes, but no, the uncertainty principle gives the width. Another thought: in some contexts, for two states, the resolution might depend on the difference in widths, but I think for basic quantum mechanics, it's the energy uncertainty that matters. The problem says "clearly distinguish these two energy levels", so it's about the energy separation. I think C is correct. But let me check the calculation once more. $\hbar = 6.582 \times 10^{-16}$ eV·s $\tau_1 = 10^{-9}$ s $\Delta E_1 = 6.582 \times 10^{-16} / 1 \times 10^{-9} = 6.582 \times 10^{-7}$ eV 6.582×10^{-7} is 0.6582×10^{-6}, so approximately 10^{-6} eV. 10^{-4} eV is 100 times larger. Yes. If I use the formula without the constant, the order of magnitude. The uncertainty $\Delta E \propto 1/\tau$. $\tau_1 = 10^{-9}$, so $\Delta E_1 \propto 10^9$ $\tau_2 = 10^{-8}$, $\Delta E_2 \propto 10^8$ So ΔE_1 is about 10 times larger than ΔE_2. So larger uncertainty is about 10^9 times \hbar, but in eV. Since \hbar is fixed, ΔE_1 is 10 times larger than ΔE_2. But in terms of the value, $\Delta E_1 \approx 10^{-6}$ eV. Options: A 10^{-9}, B 10^{-8}, C 10^{-4}, D 10^{-11} 10^{-4} is the only one larger than 10^{-6}. 10^{-8} is smaller than 10^{-6}, since $10^{-8} = 0.00000001$, $10^{-6} = 0.000001$, so 10^{-6} is larger. Yes, $10^{-6} > 10^{-8}$. So ΔE must be $> 10^{-6}$ eV, so only C is greater than that. Therefore, the answer should be C. I think that's it. ANSWER: C</p>
5	<p>Question: Answer the following multiple choice question. The last line of your response should be of the following format: 'ANSWER: \$LETTER' (without quotes) where LETTER is one of A,B,C,D. Think step by step before answering.</p> <p>Two quantum states with energies E_1 and E_2 have a lifetime of 10^{-9} sec and 10^{-8} sec, respectively. We want to clearly distinguish these two energy levels. Which one of the following options could be their energy difference so that they can be clearly resolved?</p> <p>Options: A) 10^{-9} eV B) 10^{-8} eV C) 10^{-4} eV D) 10^{-11} eV</p> <p>Model Answer: C Correct Answer: C Character Count: 6662.0</p> <p>Full Answer: First, the question is about distinguishing two quantum states with different lifetimes. The lifetimes are given: E_1 has a lifetime of 10^{-9} seconds, and E_2 has a lifetime of 10^{-8} seconds. I need to find which energy difference would allow us to clearly resolve these two levels.</p> <p>I recall that in quantum mechanics, the energy uncertainty is related to the lifetime of the state via the Heisenberg uncertainty principle. The uncertainty in energy, ΔE, is approximately related to the lifetime τ by $\Delta E \cdot \tau \approx \hbar$, where \hbar is the reduced Planck's constant.</p> <p>The Heisenberg uncertainty principle for energy and time is often written as $\Delta E \cdot \Delta t \geq \hbar/2$, but for practical purposes in spectroscopy, we use $\Delta E \approx \hbar/\tau$, where τ is the lifetime.</p>

Continued on next page

Table 7 – *Continued from previous page*

ID	Content
5	<p>So, for each state, we can find the energy width due to the finite lifetime. For state E_1, lifetime $\tau_1 = 10^{-9}$ s, so $\Delta E_1 \approx \hbar/\tau_1$. Similarly, for state E_2, $\tau_2 = 10^{-8}$ s, so $\Delta E_2 \approx \hbar/\tau_2$. Now, the energy difference between the two states, let's call it $\Delta E = E_1 - E_2$ (in magnitude), needs to be larger than the sum of the energy widths to be resolved. That is, for two peaks to be distinguishable, the energy difference should be greater than the full width at half maximum (FWHM) or something similar. In spectroscopy, if the energy difference is much larger than the individual linewidths, they can be resolved. The linewidth Γ for a state is $\Gamma = \hbar/\tau$, so the uncertainty in energy is Γ. To resolve two energy levels, the energy difference ΔE should be greater than the sum of the two linewidths, or at least comparable to the larger linewidth. Typically, for clear resolution, $\Delta E \gg \Gamma_1$ and $\Delta E \gg \Gamma_2$, but since Γ_1 and Γ_2 are different, we need ΔE to be larger than the larger of the two widths. Let me calculate the linewidths. First, $\hbar = h/(2\pi)$, and $h = 4.135667662 \times 10^{-15}$ eV·s (I think that's the value in eV seconds). I should use consistent units. Since the options are in eV, I'll work in eV. \hbar in eV·s is approximately 6.582×10^{-16} eV·s. Let me confirm. $\hbar = 4.135667662 \times 10^{-15}$ eV·s (this is h, not \hbar) $\hbar = h/(2\pi) = (4.135667662 \times 10^{-15})/(6.283185307) \approx 6.582 \times 10^{-16}$ eV·s. Yes. So $\hbar \approx 6.582 \times 10^{-16}$ eV·s. Now, for state 1: $\tau_1 = 10^{-9}$ s $\Gamma_1 = \hbar/\tau_1 = (6.582 \times 10^{-16})/(10^{-9}) = 6.582 \times 10^{-7}$ eV. Similarly, for state 2: $\tau_2 = 10^{-8}$ s $\Gamma_2 = \hbar/\tau_2 = (6.582 \times 10^{-16})/(10^{-8}) = 6.582 \times 10^{-8}$ eV. So $\Gamma_1 \approx 6.58 \times 10^{-7}$ eV. $\Gamma_2 \approx 6.58 \times 10^{-8}$ eV. The larger linewidth is $\Gamma_1 \approx 6.6 \times 10^{-7}$ eV. To clearly distinguish the two energy levels, the energy difference ΔE should be much larger than the larger linewidth, so that the peaks don't overlap significantly. In the context of the question, "clearly resolve" probably means that ΔE is greater than the sum of the linewidths or at least comparable to the larger one. Typically, for two lines to be resolved, the energy difference should be greater than the FWHM of the broader line. Since Γ_1 is larger than Γ_2, we need $\Delta E > \Gamma_1$. Let me see the options: A) 10^{-9} eV B) 10^{-8} eV C) 10^{-4} eV D) 10^{-11} eV. Now, $\Gamma_1 \approx 6.6 \times 10^{-7}$ eV, which is about 0.66×10^{-6} eV. So 10^{-6} eV is 100 times larger than 10^{-7}, but let's compare numerically. $\Gamma_1 = 6.58 \times 10^{-7}$ eV. Option A: 10^{-9} eV = 0.001×10^{-6} eV = 10^{-9} eV. 10^{-9} is much smaller than 10^{-7}, since $10^{-9}/10^{-7} = 10^{-2}$, so 100 times smaller. Option B: 10^{-8} eV = 0.1×10^{-7} eV, still smaller than Γ_1 (which is $\sim 6.6 \times 10^{-7}$, so 10^{-8} is 10 times smaller than 10^{-7}, but Γ_1 is 6.6×10^{-7}, so 10^{-8} is $0.1 \times 10^{-7} = 10^{-8}$, while Γ_1 is $6.6 \times 10^{-7} = 66 \times 10^{-8}$, so Γ_1 is about 66 times larger than 10^{-8} eV). Let's do it properly. $\Gamma_1 = 6.58 \times 10^{-7}$ eV. Option A: 10^{-9} eV = 0.001×10^{-6} eV, but better to write in same exponent. 10^{-9} eV vs 10^{-7} eV: 10^{-9} is 100 times smaller than 10^{-7}. Specifically, $\Gamma_1/(10^{-9}) = 6.58 \times 10^{-7}/1 \times 10^{-9} = 658$, so Γ_1 is 658 times larger than option A. Similarly, option B: 10^{-8} eV. $\Gamma_1/(10^{-8}) = 6.58 \times 10^{-7}/1 \times 10^{-8} = 65.8$, so Γ_1 is about 66 times larger than option B. Option C: 10^{-4} eV. $\Gamma_1/(10^{-4}) = 6.58 \times 10^{-7}/1 \times 10^{-4} = 6.58 \times 10^{-3}$, so Γ_1 is 0.00658 times 10^{-4}, meaning 10^{-4} is much larger than Γ_1. 10^{-4} eV = 0.0001 eV. $\Gamma_1 = 0.000000658$ eV, so yes, 10^{-4} is 1000 times larger than Γ_1? Let's see: $10^{-4}/\Gamma_1 = 10^{-4}/(6.58 \times 10^{-7}) = 10^{-4}/6.58 \times 10^{-7} = (1/6.58) \times 10^3 \approx 0.152 \times 1000 = 152$. So 10^{-4} eV is about 152 times larger than Γ_1. Option D: 10^{-11} eV, which is much smaller than Γ_1.</p>

Continued on next page

Table 7 – *Continued from previous page*

ID	Content
5	<p>So, for clear resolution, we need ΔE to be larger than Γ_1, the larger linewidth. Option C is 10^{-4} eV, which is larger than Γ_1 (since $\Gamma_1 \approx 10^{-6.2}$ eV, roughly 6.6×10^{-7}, so 10^{-4} is 1000 times larger? Wait no: $10^{-4} = 0.0001$ $\Gamma_1 = 0.000000658 = 6.58 \times 10^{-7}$ So $10^{-4}/\Gamma_1 = 10^{-4}/6.58 \times 10^{-7} = 1000/6.58 \approx 152$, so yes, about 152 times larger. Option B is 10^{-8} eV, which is smaller than Γ_1. $\Gamma_1 = 6.58 \times 10^{-7}$, $10^{-8} = 0.00000001$, so $\Gamma_1/10^{-8} = 65.8$, so Γ_1 is 65.8 times larger than option B. Similarly, option A is even smaller. Option D is 10^{-11}, way smaller. So only option C is larger than Γ_1. But is that sufficient? The question says "clearly distinguish these two energy levels." I think in spectroscopy, for two lines to be resolved, the energy difference should be greater than the sum of the half-widths or something. In the context of the uncertainty principle, the natural linewidth is Γ, and for two states to be distinguishable, the energy difference should be much larger than the larger linewidth. Moreover, since the states have different lifetimes, their widths are different, but the resolution criterion is often $\Delta E > \Gamma_{\max}$. Let me think if there's a standard formula. Another way to think: the energy difference must be larger than the minimum resolvable difference. The uncertainty principle gives the intrinsic width, so if ΔE is smaller than Γ_1, the two levels would be indistinguishable because the width of the first state is Γ_1, so it's spread over an energy range of about Γ_1, so if the difference is less than Γ_1, it might be within the spread. Specifically, for the two levels to be resolved, we need $E_1 - E_2 > \Gamma_1$ and $E_1 - E_2 > \Gamma_2$, but since $\Gamma_1 > \Gamma_2$, it's sufficient to have $E_1 - E_2 > \Gamma_1$. In this case, Γ_1 is about 6.6×10^{-7} eV, so we need $\Delta E > 6.6 \times 10^{-7}$ eV. Option C is 10^{-4} eV = 0.0001 eV = 1×10^{-4} eV, which is 100 times larger than 1×10^{-6}? $1 \times 10^{-4} = 100,000 \times 10^{-9}$, but $\Gamma_1 = 6.6 \times 10^{-7} = 0.66 \times 10^{-6}$. $1 \times 10^{-4} = 100 \times 10^{-6}$, $\Gamma_1 = 0.66 \times 10^{-6}$, so yes, $100 \times 10^{-6}/0.66 \times 10^{-6} \approx 151.5$, so about 150 times larger. Option B is 1×10^{-8} eV, which is 0.01×10^{-6}, while Γ_1 is 0.66×10^{-6}, so Γ_1 is about 66 times larger than option B. So if ΔE is 10^{-8} eV, it's smaller than Γ_1, so the two peaks would overlap significantly. Similarly, for option C, it's larger, so they should be resolved. But let me check the options again. Option C is 10^{-4} eV, which is 0.0001 eV. Is there a trick here? The question says: "we want to clearly distinguish these two energy levels." And the states have energies E_1 and E_2, with lifetimes given. But in quantum mechanics, the energy levels themselves might be degenerate or something, but I think here it's about the transition energies or something? No, it says "energy levels" with energies E_1 and E_2. Perhaps it's about the energy difference between them. Another thought: in the context of the uncertainty principle, the energy difference must be such that it's not affected by the broadening. I recall that for two states to be resolved, the energy difference should be greater than the sum of the decay widths. The sum $\Gamma_1 + \Gamma_2 \approx 6.58 \times 10^{-7} + 6.58 \times 10^{-8} = 7.24 \times 10^{-7}$ eV. Still, option C is 1×10^{-4}, which is much larger. Option B is 1×10^{-8}, which is less than both. But let's see the answer choices; D is 10^{-11}, which is tiny. Perhaps I misremembered the uncertainty principle. Is it $\Delta E \cdot \tau = \hbar$ or $\hbar/2$? In many contexts, the natural linewidth is $\Gamma = \hbar/\tau$, so for a state with lifetime τ, the energy uncertainty is \hbar/τ. Yes. Sometimes it's given as the full width at half maximum (FWHM) is $\Gamma = \hbar/\tau$. So I think that's standard. Perhaps the question is about the energy difference for the transition, but it says "energy levels" with energies E_1 and E_2.</p>

Continued on next page

Table 7 – *Continued from previous page*

ID	Content
5	<p>Another angle: if the two energy levels are close, they might mix, but I think for resolution, it's about the width.</p> <p>Let me see if there's a specific formula for resolution.</p> <p>In spectroscopy, the Rayleigh criterion for resolution is that the energy difference should be greater than the FWHM of the broader line.</p> <p>Here, the broader line has $\Gamma_1 = \hbar/\tau_1 = \hbar/10^{-9}$</p> <p>Since $\tau_1 < \tau_2$, $\Gamma_1 > \Gamma_2$, so Γ_1 is larger.</p> <p>So $\Delta E > \Gamma_1$ for clear resolution.</p> <p>$\Gamma_1 = \hbar/\tau_1$</p> <p>$\hbar \approx 6.58 \times 10^{-16} \text{ eV}\cdot\text{s}$</p> <p>$\tau_1 = 1 \times 10^{-9} \text{ s}$</p> <p>$\Gamma_1 = 6.58 \times 10^{-16}/1 \times 10^{-9} = 6.58 \times 10^{-7} \text{ eV}$</p> <p>Now, options:</p> <p>A) $1 \times 10^{-9} \text{ eV} \rightarrow$ too small</p> <p>B) $1 \times 10^{-8} \text{ eV} \rightarrow 1 \times 10^{-8} < 6.58 \times 10^{-7}$? $1 \times 10^{-8} = 0.1 \times 10^{-7}$, $6.58 \times 10^{-7} = 65.8 \times 10^{-8}$, so $65.8 \times 10^{-8} > 1 \times 10^{-8}$, yes, so smaller</p> <p>C) $1 \times 10^{-4} \text{ eV} = 100 \times 10^{-6} \text{ eV}$, while $\Gamma_1 = 0.658 \times 10^{-6} \text{ eV}$, so $100 \times 10^{-6} > 0.658 \times 10^{-6}$, yes</p> <p>D) $1 \times 10^{-11} \text{ eV} \rightarrow$ way smaller</p> <p>So only C is larger than Γ_1.</p> <p>But let me check if the question is tricky.</p> <p>The lifetimes are for the states, but when we say "distinguish these two energy levels", it might be in a measurement context.</p> <p>Perhaps the energy difference must be such that the time it takes to resolve is related.</p> <p>Another thought: the minimum resolvable energy difference is on the order of \hbar/τ, but for two states, it might be different.</p> <p>I recall that in the context of the uncertainty principle, the energy difference ΔE must satisfy $\Delta E > \hbar/\tau$ for some τ, but here we have two different τ.</p> <p>I think my initial approach is correct.</p> <p>Let me calculate numerically.</p> <p>$\hbar = 1.0545718 \times 10^{-34} \text{ J}\cdot\text{s}$</p> <p>But in eV, $\hbar = 6.582 \times 10^{-16} \text{ eV}\cdot\text{s}$, as I had.</p> <p>$\tau_1 = 10^{-9} \text{ s}$</p> <p>$\Gamma_1 = \hbar/\tau_1 = 6.582 \times 10^{-16}/1 \times 10^{-9} = 6.582 \times 10^{-7} \text{ eV}$</p> <p>Similarly, $\tau_2 = 10^{-8} \text{ s}$, $\Gamma_2 = 6.582 \times 10^{-16}/1 \times 10^{-8} = 6.582 \times 10^{-8} \text{ eV}$</p> <p>So $\Gamma_{\max} = \Gamma_1 = 6.582 \times 10^{-7} \text{ eV}$</p> <p>For clear resolution, ΔE should be greater than, say, 10 times Γ_{\max} or something? But typically, if it's a factor of 2 or 3, it might be barely resolved, but for "clearly distinguish", it should be significantly larger.</p> <p>In multiple choice, option C is 10^{-4} eV, which is about 150 times larger than Γ_1.</p> <p>Option B is 10^{-8} eV, which is about 66 times smaller than Γ_1.</p> <p>So if $\Delta E = 10^{-8} \text{ eV}$, and $\Gamma_1 = 6.58 \times 10^{-7} \text{ eV}$, then the relative difference is $(10^{-8})/(6.58 \times 10^{-7}) \approx 0.015$, so 1.5</p> <p>Whereas for C, it's 150 times larger, so very clear.</p> <p>Option D is even smaller.</p> <p>But is there a possibility that I have the uncertainty principle wrong?</p> <p>Sometimes people use the time-energy uncertainty as $\Delta E \Delta t \geq \hbar/2$, so the minimum uncertainty is $\hbar/2$, but for lifetime, it's often approximated as $\Delta E \approx \hbar/\tau$.</p> <p>In many textbooks, for the natural linewidth, $\Gamma = \hbar/\tau$.</p> <p>For example, in the context of the uncertainty principle for decay, the energy width is \hbar/τ.</p> <p>So I think it's correct.</p> <p>Perhaps the question is about the energy difference for the transition between them, but it says "energy levels" with energies E_1 and E_2.</p> <p>Another interpretation: if the two energy levels are close, they might not be distinct because of broadening.</p> <p>But the question is: "we want to clearly distinguish these two energy levels" meaning that we want to see them as separate lines.</p> <p>So yes, the energy difference must be larger than the linewidths.</p> <p>Moreover, looking at the options, D is 10^{-11} eV, which is extremely small, while the lifetimes are given in seconds, so it should be larger.</p> <p>Let me see the answer choices; C is 10^{-4} eV, which seems reasonable.</p> <p>But let me see if there's a calculation mistake.</p>

Continued on next page

Table 7 – *Continued from previous page*

ID	Content
5	<p>$\tau_1 = 10^{-9}$ s, so $\Gamma_1 = \hbar/\tau_1$ \hbar in eV·s is about 6.58×10^{-16} $\Gamma_1 = 6.58 \times 10^{-16}/1 \times 10^{-9} = 6.58 \times 10^{-7}$ eV 10^{-7} eV is 0.0000001 eV, Γ_1 is 0.000000658 eV. Option B is 10^{-8} eV = 0.00000001 eV, which is smaller. Option C is 10^{-4} eV = 0.0001 eV. Yes. Perhaps the question is about the energy difference in terms of the uncertainty. Another thought: in some contexts, for two states to be distinguishable, the energy difference should be greater than the uncertainty of each, but since they have different uncertainties, we take the larger one. I think C is correct. But let me see why the other options might be tempting. Option D is 10^{-11} eV, which is smaller than Γ_1 by a factor of about 60,000, so no. Option A is 10^{-9}, even smaller. Option B is 10^{-8}, which is close to Γ_2 but smaller than Γ_1. Γ_2 is 6.58×10^{-8}, so 10^{-8} is about 0.658 times Γ_2? $10^{-8}/6.58 \times 10^{-8} \approx 0.152$, so about 15 Whereas for C, it's large. Perhaps the question is misstated, but I think C is the answer. I recall that in some multiple-choice questions, they use the formula directly. For example, the energy difference must be at least on the order of \hbar/τ, and since τ is 10^{-9} s for the first state, $\hbar/\tau \approx 10^{-6}$ eV or something. $\hbar/\tau_1 = 6.58 \times 10^{-7}$ eV, which is about 10^{-6} eV (since 10^{-6} is 1×10^{-6}, 6.58×10^{-7} is 0.658×10^{-6}). Options: A is 10^{-9}, B 10^{-8}, C 10^{-4}, D 10^{-11} 10^{-4} is 100 times larger than 10^{-6}, so it's fine. 10^{-8} is 100 times smaller than 10^{-6}. So yes. Perhaps they expect us to compute \hbar/τ for the shorter lifetime. The shortest lifetime is $\tau_1 = 10^{-9}$ s, so Γ_1 is largest. So $\Delta E > \hbar/\tau_1$ Now, $\hbar/\tau_1 \approx 6.6 \times 10^{-7}$ eV Which is closest to 10^{-6} eV, but the options don't have 10^{-6}, they have 10^{-4} and 10^{-8}. 10^{-4} is 100 times larger, but it's the only one larger. 10^{-8} is smaller. So in multiple choice, C is the only one that is larger. Option B is 10^{-8}, which is smaller than Γ_1. Unless I miscalculated \hbar. Let me double-check \hbar in eV·s. $h = 4.135667662 \times 10^{-15}$ eV·s (Planck's constant) $\hbar = h/(2\pi) = 4.135667662 \times 10^{-15}/6.283185307 \approx?$ $4.135667662 \times 10^{-15}/6.283185307 \approx (4.135667662/6.283185307) \times 10^{-15} \approx 0.6582 \times 10^{-15} = 6.582 \times 10^{-16}$ eV·s. Yes. $\tau_1 = 10^{-9}$ s $\Gamma_1 = 6.582 \times 10^{-16}/1 \times 10^{-9} = 6.582 \times 10^{-7}$ eV Yes. 10^{-7} eV is 0.0000001 eV, Γ_1 is 0.0000006582 eV. Option C: $10^{-4} = 0.0001$ eV, which is 1000 times larger? $0.0001/0.0000006582 \approx 152$, so about 150 times. In spectroscopy, for two lines to be resolved, the energy difference should be greater than the FWHM of the broader line, which is Γ_1 here. So C should be correct. Perhaps the question is about the energy difference for the transition, but it says "energy levels" with energies E_1 and E_2. Another interpretation: if the two energy levels are degenerate or something, but I think not. Perhaps "clearly distinguish" means that the energy difference is much larger than the uncertainty. I think I'm overcomplicating. Let me see the answer choices; D is 10^{-11} eV, which is way too small. For example, if ΔE were 10^{-11} eV, and Γ_1 is 10^{-6} eV, then ΔE is 100,000 times smaller, so completely unresolved.</p>

Continued on next page

Table 7 – *Continued from previous page*

ID	Content
5	<p>Similarly, B is 10^{-8}, which is 60 times smaller than Γ_1. C is 150 times larger. So C is the only reasonable choice. Perhaps they want the difference to be at least $\hbar/(\tau_1 + \tau_2)$ or something, but that doesn't make sense. Or the minimum resolvable difference is \hbar/τ for the shortest lifetime. I think C is correct. So I'll go with C. But let me see the options again. A) 10^{-9} eV B) 10^{-8} eV C) 10^{-4} eV D) 10^{-11} eV Yes. In some contexts, for time-energy, but I think it's fine. So the answer should be C. The question says "which one of the following options could be their energy difference so that they can be clearly resolved?" And C is 10^{-4} eV. Perhaps they expect a calculation without numbers. For example, $\Gamma_1 \approx \hbar/\tau_1$, $\tau_1 = 10^{-9}$ s $\hbar \approx 10^{-15}$ eV·s (roughly, since 6.58×10^{-16} is about 10^{-15}) So $\Gamma_1 \approx 10^{-15}/10^{-9} = 10^{-6}$ eV Similarly, $\Gamma_2 \approx 10^{-15}/10^{-8} = 10^{-7}$ eV So $\Gamma_{\max} \approx 10^{-6}$ eV Then $\Delta E > 10^{-6}$ eV for clear resolution. Options: A 10^{-9}, B 10^{-8}, C 10^{-4}, D 10^{-11} 10^{-4} is 100 times larger than 10^{-6}, so it works. 10^{-8} is 100 times smaller than 10^{-6}. So yes. Therefore, the answer is C. I think that's it. To determine which energy difference allows clear distinction between two quantum states with lifetimes of 10^{-9} seconds and 10^{-8} seconds, the energy uncertainty due to the finite lifetime must be considered. According to the Heisenberg uncertainty principle, the energy uncertainty ΔE for a state with lifetime τ is approximately $\Delta E \approx \hbar/\tau$, where \hbar is the reduced Planck's constant ($\hbar \approx 6.582 \times 10^{-16}$ eV · s). For the state with lifetime $\tau_1 = 10^{-9}$ s: $\Gamma_1 = \frac{\hbar}{\tau_1} = \frac{6.582 \times 10^{-16}}{10^{-9}} = 6.582 \times 10^{-7}$ eV For the state with lifetime $\tau_2 = 10^{-8}$ s: $\Gamma_2 = \frac{\hbar}{\tau_2} = \frac{6.582 \times 10^{-16}}{10^{-8}} = 6.582 \times 10^{-8}$ eV The larger energy uncertainty is $\Gamma_1 \approx 6.582 \times 10^{-7}$ eV. To clearly resolve two energy levels, the energy difference ΔE must be significantly larger than the larger uncertainty Γ_1 (typically by a factor of at least 10-100 for clear distinction). Now, evaluate the options: - A) 10^{-9} eV: $10^{-9}/6.582 \times 10^{-7} \approx 0.0015$, so ΔE is about 0.15- B) 10^{-8} eV: $10^{-8}/6.582 \times 10^{-7} \approx 0.015$, so ΔE is about 1.5- C) 10^{-4} eV: $10^{-4}/6.582 \times 10^{-7} \approx 152$, so ΔE is about 152 times larger than Γ_1—sufficient for clear resolution. - D) 10^{-11} eV: $10^{-11}/6.582 \times 10^{-7} \approx 0.000015$, so ΔE is about 0.0015 Only option C satisfies the condition for clear resolution, as it is much larger than the larger energy uncertainty Γ_1. ANSWER: C</p>

Table 8: Detailed individual metrics for different merging granularities (full data).

ID	Method	f1 (↑)	f2 (↑)	GPQA_ACC (↑)	GPQA_TOKENS (↓)	AIME25_ACC (↑)	AIME25_TOKENS (↓)	Pareto
0	Layer-wise	0.8698	0.8047	0.6212	4037	0.7666	8891	✓
1		0.9527	0.2414	0.6616	9136	0.7666	15496	✗
2		0.3656	1.0585	0.4545	791	0.6666	7321	✓
3		0.6848	0.8697	0.6364	3427	0.6333	8161	✓
4		0.3428	1.0599	0.4697	958	0.6333	7037	✓
5		0.1783	1.0666	0.4949	764	0.5000	7158	✓
6		0.2116	1.0600	0.4848	717	0.5333	7392	✓
7		0.8826	0.7393	0.6010	4308	0.8000	10132	✓
8		0.5753	1.0409	0.5303	900	0.7000	7602	✓
9		0.6101	0.9011	0.6263	2509	0.6000	8732	✓
0	Block-wise (n=18)	1.0691	0.5632	0.6919	6660	0.8000	11077	✓
1		0.6894	0.7855	0.5859	4706	0.7000	8384	✗
2		0.5086	1.0210	0.5505	1573	0.6333	7106	✗
3		0.7308	0.7012	0.6061	5104	0.7000	9912	✗
4		0.1266	1.0383	0.4697	981	0.5000	7545	✗
5		0.5455	0.9135	0.6212	2698	0.5666	8140	✗
6		0.8677	0.6257	0.6465	6076	0.7333	10369	✗
7		0.7183	0.7383	0.6263	3923	0.6667	10729	✗
8		0.8552	0.6671	0.6667	5376	0.7000	10366	✗
0	Block-wise (n=9)	0.9320	0.4935	0.6515	7576	0.7666	11472	✗
1		0.9735	0.3001	0.6717	8549	0.7666	14888	✗
2		0.8552	0.5161	0.6667	7219	0.7000	11430	✗
3		0.7411	0.6215	0.6111	6391	0.7000	10008	✗
4		0.5628	0.8946	0.5505	1273	0.6667	10726	✗
5		0.6284	0.8021	0.6616	4832	0.5666	7779	✗
6		0.4776	0.9933	0.5354	1680	0.6333	7643	✗
7		1.0611	0.2645	0.6616	8242	0.8334	16240	✗
8		0.7930	0.6184	0.6364	6471	0.7000	9968	✗
9	Model-level	1.0818	0.2037	0.6717	8082	0.8334	18005	✗
10		0.3822	1.0249	0.5152	1226	0.6000	7520	✗
11		1.0715	0.2445	0.6667	8176	0.8334	16841	✗
12		1.0506	0.2790	0.6566	8406	0.8333	15631	✗
13		0.9506	0.3431	0.6869	8263	0.7333	14233	✗
0		0.4983	0.9734	0.5455	1441	0.6333	8496	✗
1		0.5168	0.9129	0.5808	3197	0.6000	7417	✗
2		0.5227	0.7743	0.6364	4966	0.5333	8279	✗
3		0.6516	0.6855	0.6465	6165	0.6000	8735	✗
4		0.5812	0.7023	0.5859	6368	0.6333	8013	✗
5		0.7700	0.6019	0.6515	7065	0.6667	9503	✗
6		0.8012	0.5726	0.6667	7220	0.6667	10008	✗
7		0.8885	0.5154	0.6566	7697	0.7333	10740	✗
8		0.8906	0.3548	0.6313	8851	0.7666	13067	✗
9	AIME25	1.0691	0.3285	0.6919	8812	0.8000	13786	✗
10		1.0923	0.3010	0.6768	8571	0.8334	14834	✓
11		1.1231	0.2153	0.6919	8443	0.8333	17178	✓
12		1.1438	0.2042	0.7020	8560	0.8333	17285	✓